Electronic Supplementary Information

Sucrose-mediated heat-stiffening microemulsion-based gel for enzyme entrapment and catalysis

Akshi Deshwal, Himanshu Chitra, Madhusudan Maity, Santanu Kumar Pal, Subhabrata Maiti*

Department of Chemical Sciences, Indian Institute of Science Education and Research (IISER) Mohali, Knowledge City, Manauli 140306, India

TABLE OF CONTENTS

1. Materials and Methods

All commercially available reagents were used as received without any further purification. All the enzymezs – Glucose Oxidase (GOx), alpha glucosidase, Horseradish Peroxidase (HRP), were procured from Sisco Research Laboratory (SRL), India. Pyrogallol was purchased from Sigma-Aldrich and H_2O_2 (30 %) and 4-nitrophenyl-α-glucopyranoside were procured from SRL, India. Other chemicals including surfactant like CTAB and alcohols like n-butanol, n-pentanol, n-hexanol, n-heptanol, n-octanol along with sugars like sucrose, glucose and fructose were also purchased from SRL, India. Stock solutions of enzymes/proteins were prepared both by weight and UV-vis spectroscopy using the molar extinction coefficients: ε_{280} (GOx from Aspergillus Niger) = 220800 $M^{-1}cm^{-1}$, ε_{280} (alpha glucosidase ex Yeast for biochemistry) = 130650 $M^{-1}cm^{-1}$, ε_{403} (HRP Peroxidase ex. Horseradish) = 102000 $M^{-1}cm^{-1}$, ε_{274} (Trypsin from bovine pancreas) = 30,290 $M^{-1}cm^{-1}$.

UV-Vis studies were performed using Varian Cary 60 (Agilent technologies) spectrophotometer. Total reaction volume in the cuvette was fixed at 1 ml and cuvette of path length 1 cm was used for the entire kinetic study. All measurements have been performed at 25 °C.

Fluorescence measurements were performed using Cary Eclipse Fluorescence Spectro-fluorometer.

The optical and fluorescence microscopic images were collected using Zeiss Axis Observer 7 microscope having AxioCam 503 Mono 3 Mega pixel with ZEN 2 software.

The Transmission Electron Microscopy images were taken on JEOL JEM-F200 microscope.

The Dynamic Light Scattering (DLS) data was recorded on Malvern Zetasizer Nano-ZS90.

Rheology data was recorded on Anton-Paar MCR 302 Rheometer.

2. Formation of Reverse Micelle in absence and presence of carbohydrate solution:

2.1. Reverse micelle formation technique:

It has been synthesized as reported in literature (reference 3 in main manuscript). CTAB (50 mM)/iso-octane/*n*-pentanol/water microemulsion system at the required *z* and W_0 values. The microstructural parameter z and W_0 have been defined as the molar ratio of [co-surfactant]/[surfactant] and [water]/[surfactant], respectively. For instance, CTAB (36.4 mg) was dispersed in isooctane in a 2 mL volumetric flask, to which the calculated amount of co-surfactant was added to attain the corresponding z (= [co-surfactant]/[surfactant]) value and shaken vigorously. Finally, water or carbohydrate solution was added (to reach the corresponding W_0), and the whole suspension was vortexed to obtain a clear homogeneous solution of CTAB (50 mM)/isooctane/n-hexanol/water or aqueous carbohydrate solution reverse micelle. Different alcohols were used as co-surfactant like butanol, pentanol, heaxanol, heptanol and octanol. W_0 range for reverse micelle formation at fixed z = 10 with different co-surfactant have been illustrated in the table given below (Table S1+S2).

2.2. W_0 range of the reverse micelle formation in absence and presence of carbohydrate solution:

Table S1. Values of W_0 range in clear reverse micelle[a] forming zone and the formation of opaque gel with different co-surfactant at fixed z = 10.

Alcohol	**W_0 range where reverse micelle forms**	**Opaque Gel formation range**
Butanol	16-60	Not formed
Pentanol	16-60	80 – 140
Hexanol	16-66	Not formed
Heptanol	16-60	Not formed
Octanol	Not formed (always cloudy)	-

[a] [CTAB] = 50 mM, [co-surfactant] = 500 mM. After mixing all the components vortexing was done for minimum 5 min to ensure visible clarity in the formed solution.

Table S2. Values of W_0 range in clear reverse micelle[a] forming zone and the formation of opaque gel in absence and presence of carbohydrate solution of different concentration (250, 500 and 1000 mM) with only n-Pentanol as co-surfactant at fixed z = 10.

Sugar	Visibility (W_0)	Opaque Gel (W_0)
Only Pentanol (no sugar)	16-60	80-140
Glucose solution [250 mM]	12-66	90-140
Fructose solution [250 mM]	12-60	90-140
Sucrose solution [250 mM]	12-84	100-144
Glucose solution [500 mM]	12-72	100-144
Fructose solution [500 mM]	12-72	100-140
Sucrose solution [500 mM]	12-84	104-144
Glucose solution [1000 mM]	12-102	120-160
Fructose solution [1000 mM]	12-90	120-150
Sucrose solution [1000 mM]	12-110	130-180 (Clear Gel)

[a] [CTAB] = 50 mM, [n-pentanol] = 500 mM. After mixing all the components vortexing was done for minimum 5 min to ensure visible clarity in the formed solution. For carbohydrate containing MBG, instead of water, aqueous carbohydrate solution of a particular concentration was added.

2.3. Optical images of inverted glass vials:

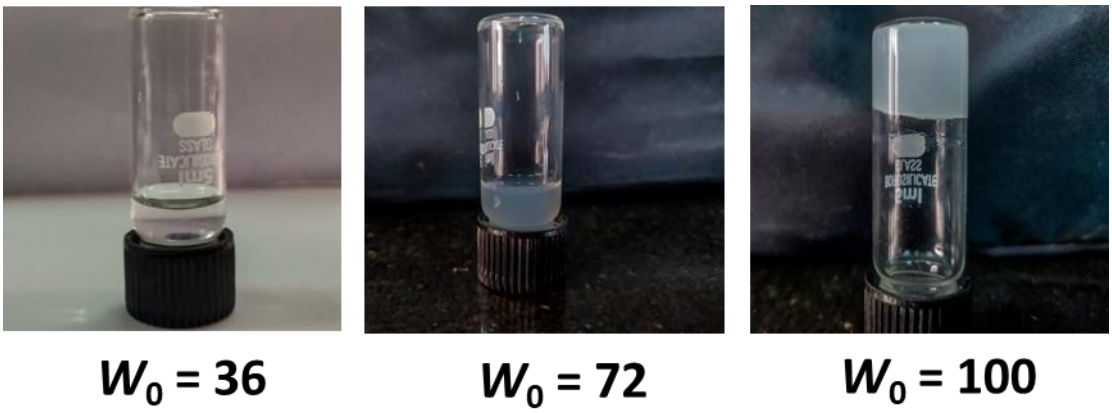

Fig. S1. Optical images of inverted vials of CTAB (50 mM)/isooctane/n-pentanol/water reverse micelles at different W_0. 5 min vortexing was done after mixing of all the components. The images clearly demonstrate that at W_0 = 100, an opaque gel was formed when *n*-pentanol was used as co-surfactant.

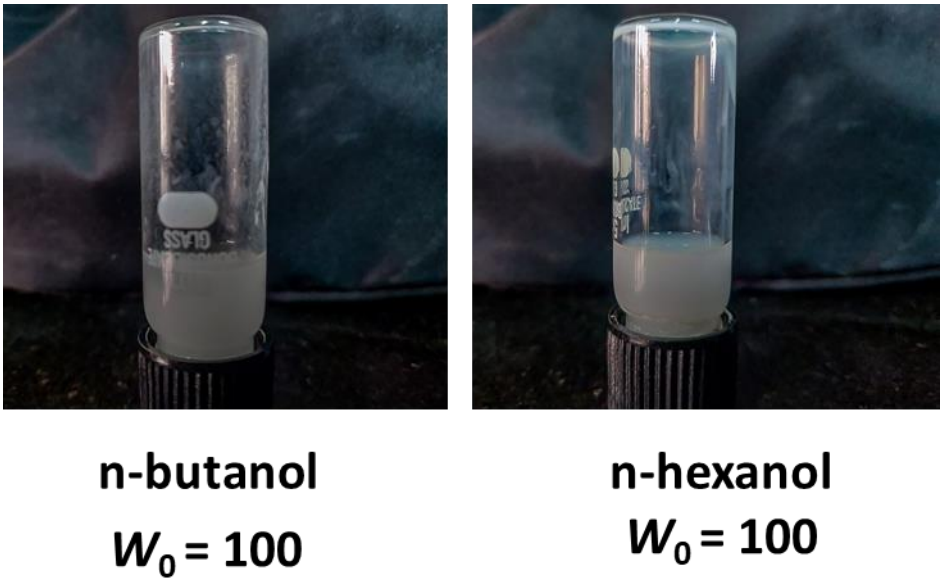

Fig. S2. Optical images of inverted vials of CTAB (50 mM)/isooctane/n-butanol or n-hexanol/water reverse micelles at W_0 = 100 . 5 min vortexing was done after mixing of all the components. The images clearly demonstrate that at W_0 = 100, no stable gel was formed when *n*-butanol and n-hexanol were used as co-surfactant.

Fig. S3. Optical images of inverted vials of CTAB (50 mM)/isooctane/n-Pentanol/sucrose solution reverse micelles at W_0 = 100 . 5 min vortexing was done after mixing of all the components. The images clearly demonstrate that at W_0 = 100, sucrose forms stable gel in presence of n-pentanol as co-surfactant.

3. Dynamic Light Scattering (DLS) Data

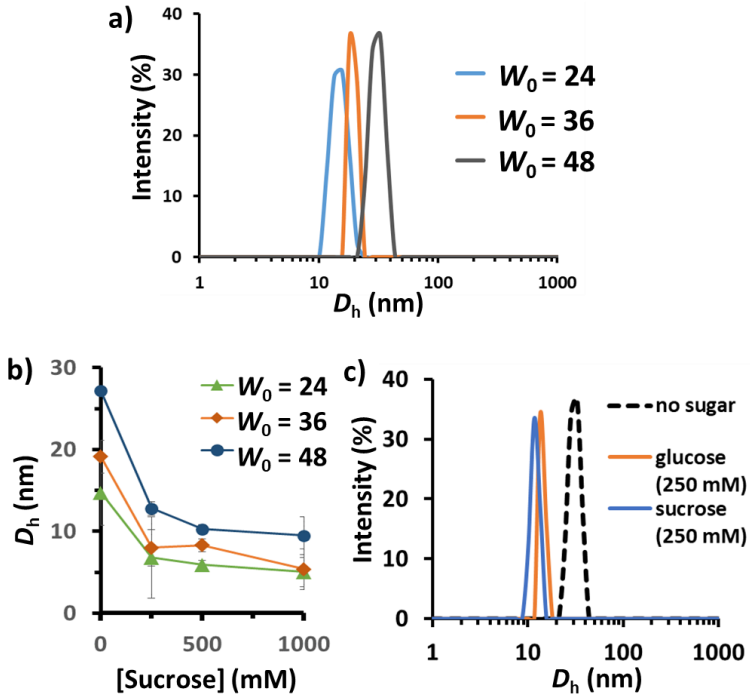

Fig. S4. (a) Representative DLS plot to show the increase in D_h with increasing W_0 in CTAB (50 mM)/isooctane/n-pentanol/water solution. (b) Hydrodynamic diameter (Dh) of reverse micelle at three different W0 (24, 36, 48) in absence and presence of sucrose solution of three different concentration (250, 500 and 1000 mM). (c) Representative DLS plot to show the decrease in Dh in presence of glucose and sucrose solution.

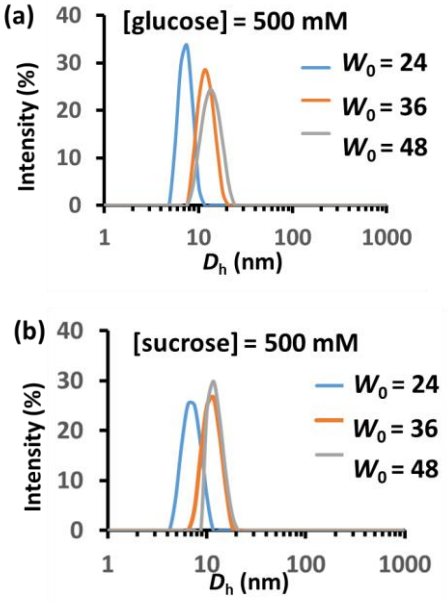

Fig. S5. Representative DLS plot to show the increase in D_h with increasing W_0 in (a) CTAB(50 mM)/isooctane/n-pentanol/500 mM glucose and (b) CTAB(50 mM)/isooctane/n-pentanol/500 mM 500 mM sucrose solution.

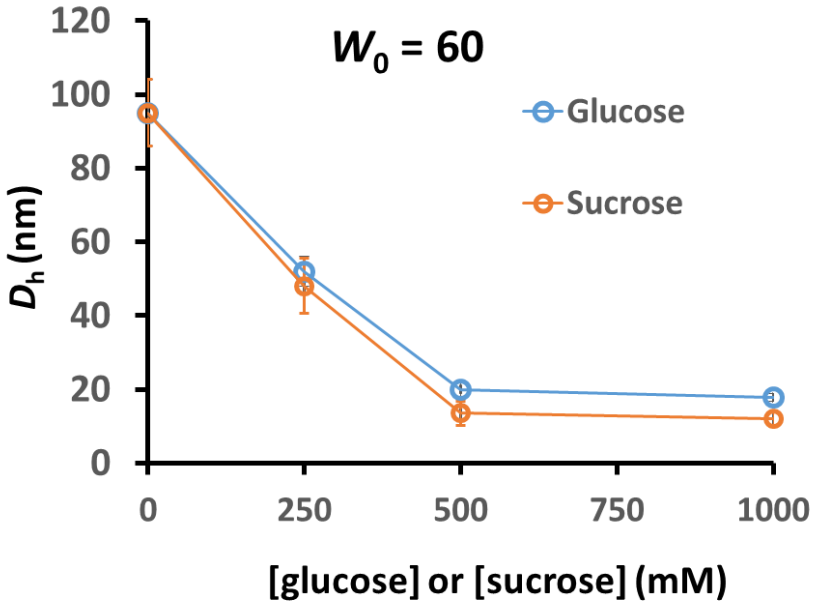

Fig. S6. Hydrodynamic diameter (D_h) of reverse micelle at W_0 = 60, in absence and presence of glucose and sucrose solution of three different concentration (250, 500 and 1000 mM).

We have measured only CTAB reverse miceller (in absence of any carbohydrate) solution at different W_0 at 24, 36 and 48) and found increasing D_h as 14.7 ± 1, 19 ± 2.1 and 27 ± 3.5 nm, respectively (Fig. S4, ESI). Addition of either glucose or sucrose resulted a considerable decrease in D_h value in each W_0 in Fig. S4. For instance, at W_0 = 24, presence of 250, 500 and 1000 mM glucose solution in the water pool resulted a decrease in D_h from 14.7 ± 1 to 7.7 ± 1.1, 6.3 ± 1.4 and 5.9 ± 0.6 nm, respectively (Fig. S4 + S5, ESI). Similar trend was also observed in sucrose solution containing reverse micelles in almost every cases. The effect of sucrose in decreasing the size becomes more prominent in higher W_0 = 60 as the D_h of the reverse micelles become 13 ± 2 and 18 ± 3 nm in presence of 500 mM sucrose and glucose solution, respectively from 95 ± 24 nm (in absence of any carbohydrate solution) (Fig. S6, ESI). Beyond W_0 = 60, DLS measurement was not possible as polydispersity index and scattering due to cloudiness of the solution were high.

4. Conductivity measurement:

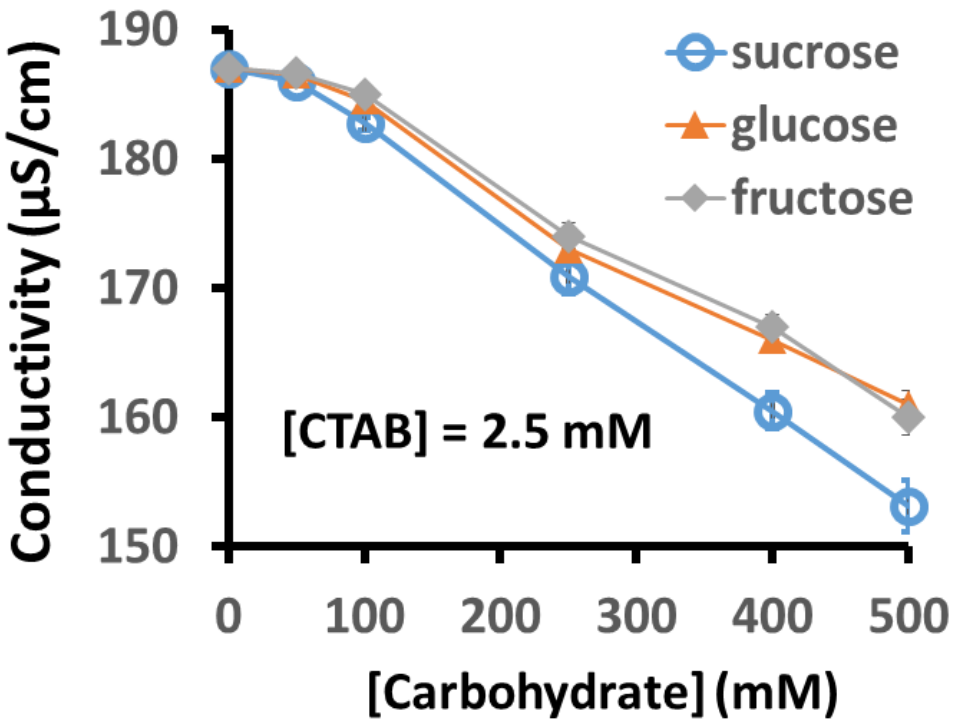

Fig. S7. Conductivity values of CTAB miceller solution (2.5 mM) as a function of the concentration of glucose, fructose and sucrose in aqueous solution. Error bars are the standard deviation of triplicate experiment. The decrease in conductivity value is due to the binding of hydroxyl group of carbohydrates and cationic headgroup of CTAB. The graph suggests that binding with sucrose and CTAB is higher than other two carbohydrates glucose and fructose.

5. Fluorescence Studies

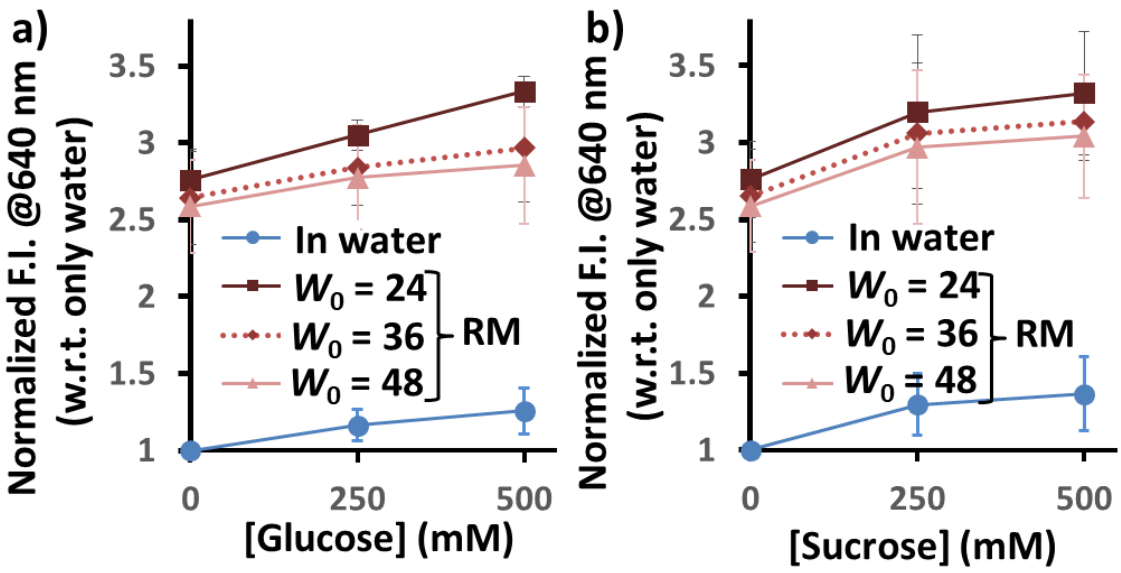

Fig. S8. Normalized fluorescence intensity (FI) (average of triplicate experiment) of crystal violet (CV) (at λ = 640 nm) excited at 575 nm with respect to FI of CV in only water in absence and presence of 250 and 500 mM (c) glucose and (d) sucrose solution in water and reverse micelle at varying W_0 (=24, 36, 48). Experimental condition: [CTAB] = 50 mM, z = 10, T = 25 °C.

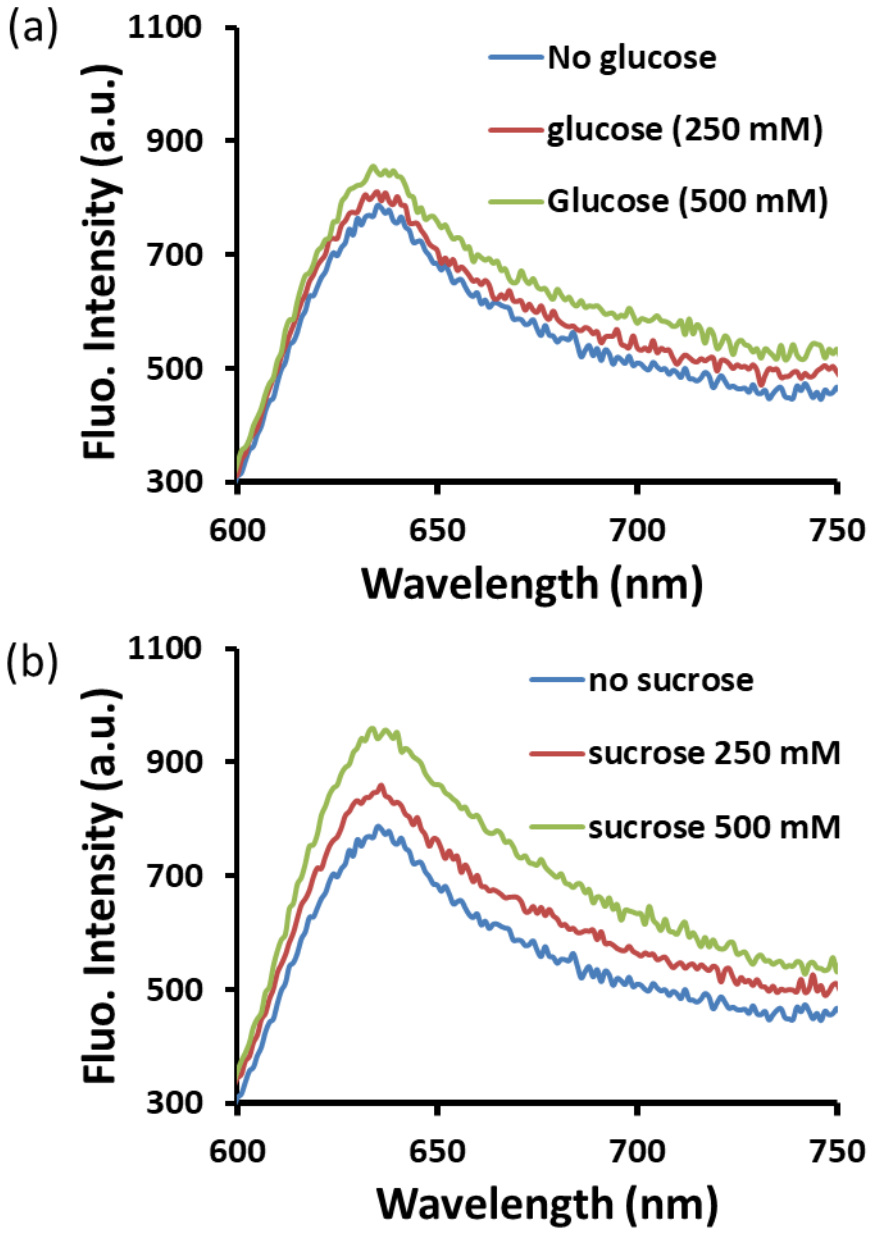

Fig. S9. Representative fluorescence spectra of crystal violet (10 µM) in absence and presence of (a) glucose and (b) sucrose solution in water. Excitation wavelength = 575 nm, excitation and emission slit width = 10 and 5 nm. T = 25 °C.

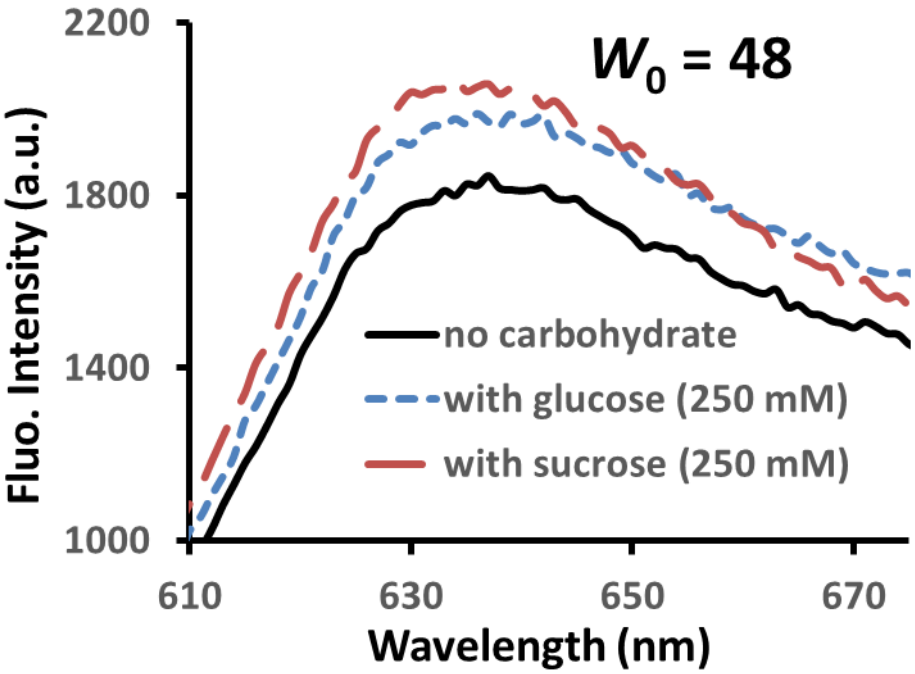

Fig. S10. Representative fluorescence spectra of crystal violet (10 µM) in absence and presence of glucose and sucrose solution (250 mM) in CTAB(50 mM)/isooctane/n-pentanol/carbohydrate solution reverse micelle at W_0 = 48. Excitation wavelength = 575 nm, excitation and emission slit width = 10 and 5 nm. T = 25 °C.

6. Rheological Studies

Below is rheology study with only water based MBG having n-pentanol as the co-surfactant.

At 60 °C, G' value at linear viscoelastic (LVE) range of MBG has increased by almost 4-fold compared to 25 °C.

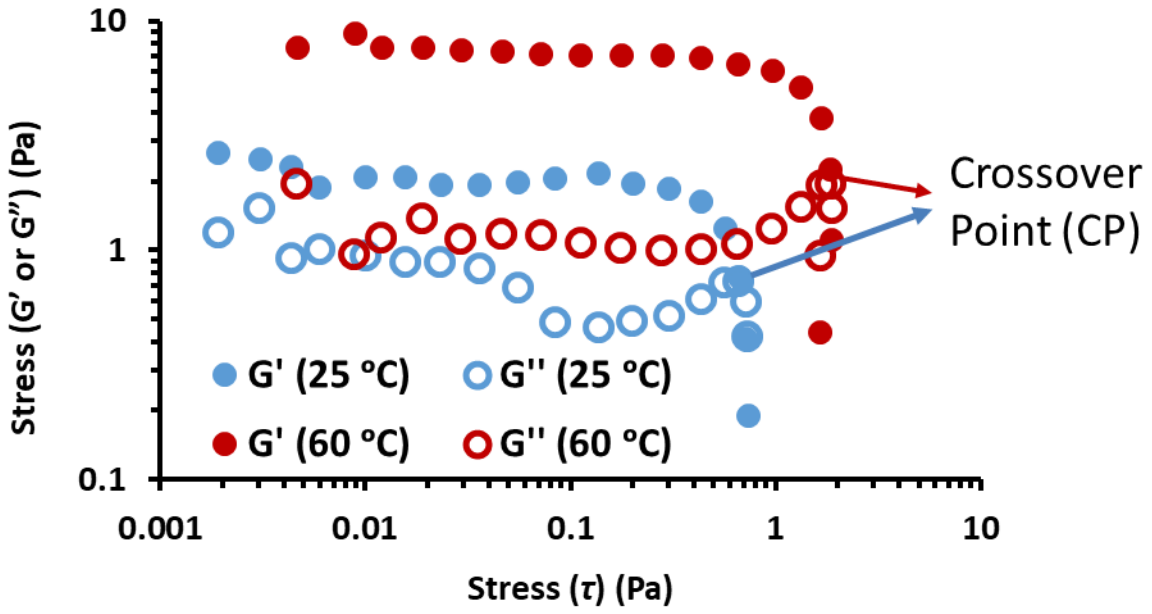

Fig. S11. Plot of storage modulus (G') and loss modulus (G") as a function of oscillatory stress at constant angular frequency (ω = 0.1 rad/s) measured with CTAB based MBG (prepared by using of only water) with n-pentanol as co-surfactant formed at T = 25 °C and 60 °C. Experimental condition: [CTAB] = 50 mM, z = 10, W_0 = 120.

Below is rheology study with sucrose solution (250 and 1000 mM) based MBG having n-pentanol as the co-surfactant.

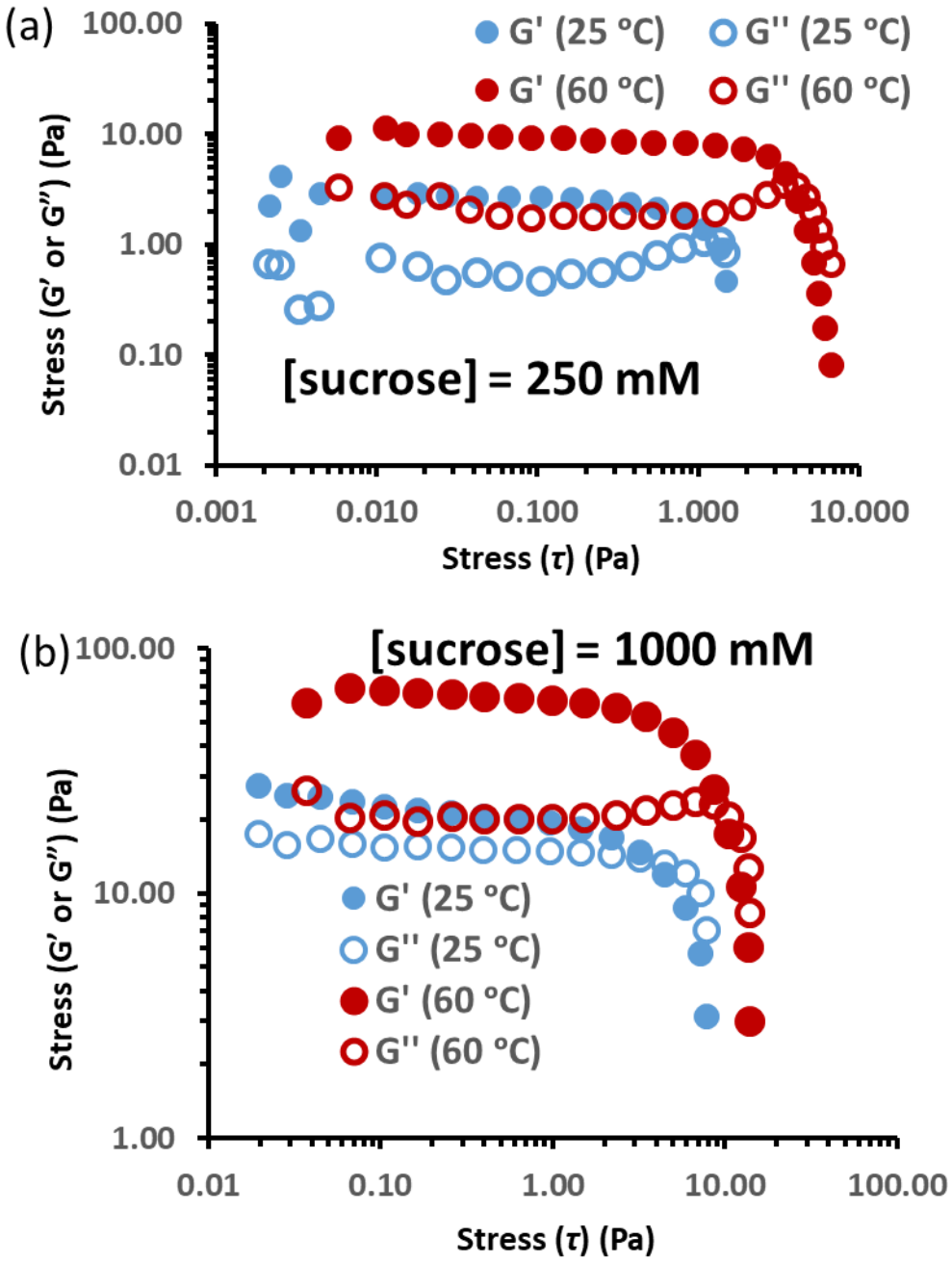

Fig. S12. Plot of storage modulus (G') and loss modulus (G") as a function of oscillatory stress at constant angular frequency (ω = 0.1 rad/s) measured with CTAB based MBG prepared with (a) sucrose (250 mM) and (b) sucrose (1000 mM) solution having n-pentanol as co-surfactant formed at T = 25 °C and 60 °C. Experimental condition: [CTAB] = 50 mM, z =10, W_0 = 120.

Below is rheology study with glucose solution (500 and 1000 mM) based MBG having n-pentanol as the co-surfactant.

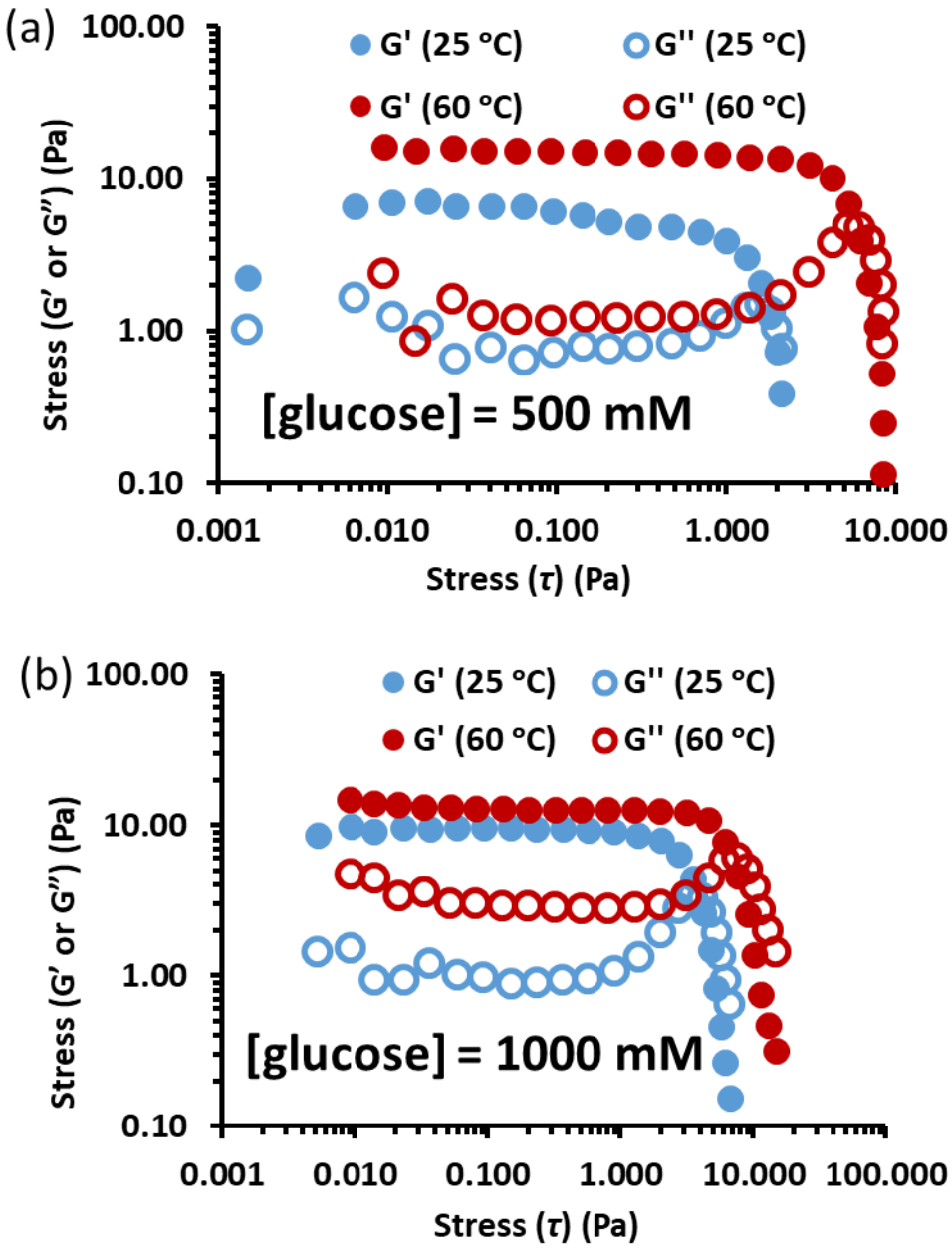

Fig. S13. Plot of storage modulus (G′) and loss modulus (G″) as a function of oscillatory stress at constant angular frequency (ω = 0.1 rad/s) measured with CTAB based MBG prepared with (a) glucose (500 mM) and (b) glucose (1000 mM) solution having n-pentanol as co-surfactant formed at T = 25 °C and 60 °C. Experimental condition: [CTAB] = 50 mM, z = 10, W_0 = 120.

Below is rheology study with fructose solution (1000 mM) based MBG having n-pentanol as the co-surfactant.

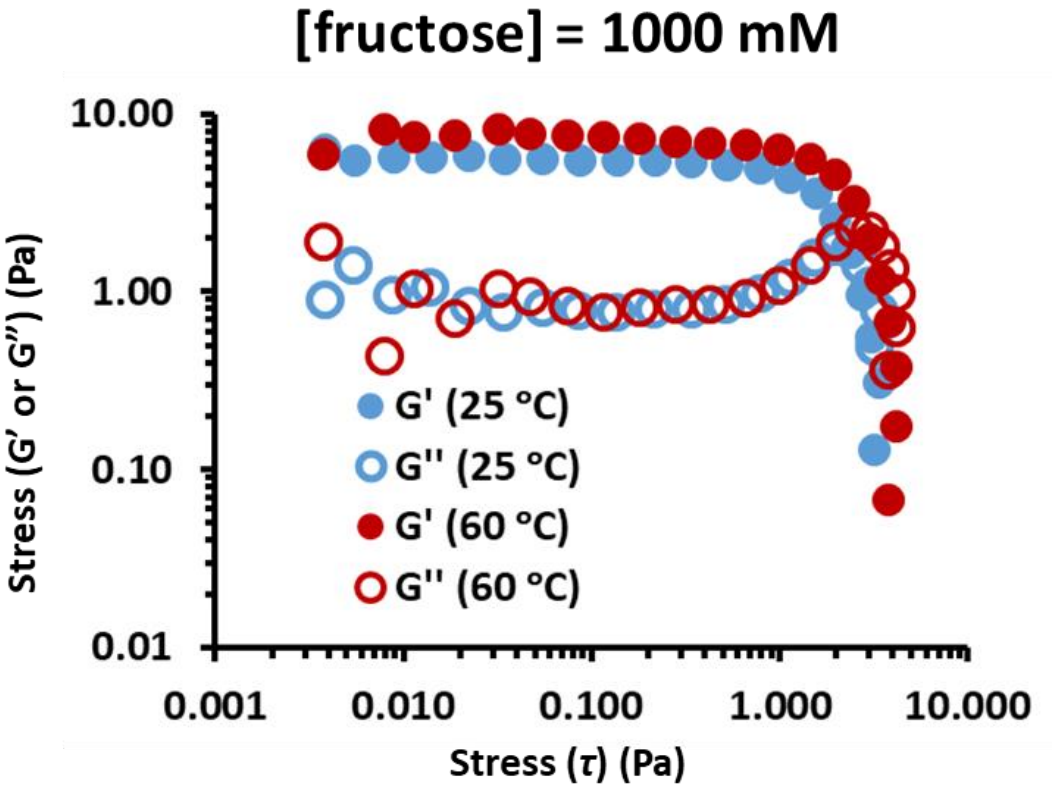

Fig. S14. Plot of storage modulus (G') and loss modulus (G") as a function of oscillatory stress at constant angular frequency (ω = 0.1 rad/s) measured with CTAB based MBG prepared with fructose (1000 mM) solution having n-pentanol as co-surfactant formed at T = 25 °C and 60 °C. Experimental condition: [CTAB] = 50 mM, z = 10, W_0 = 120.

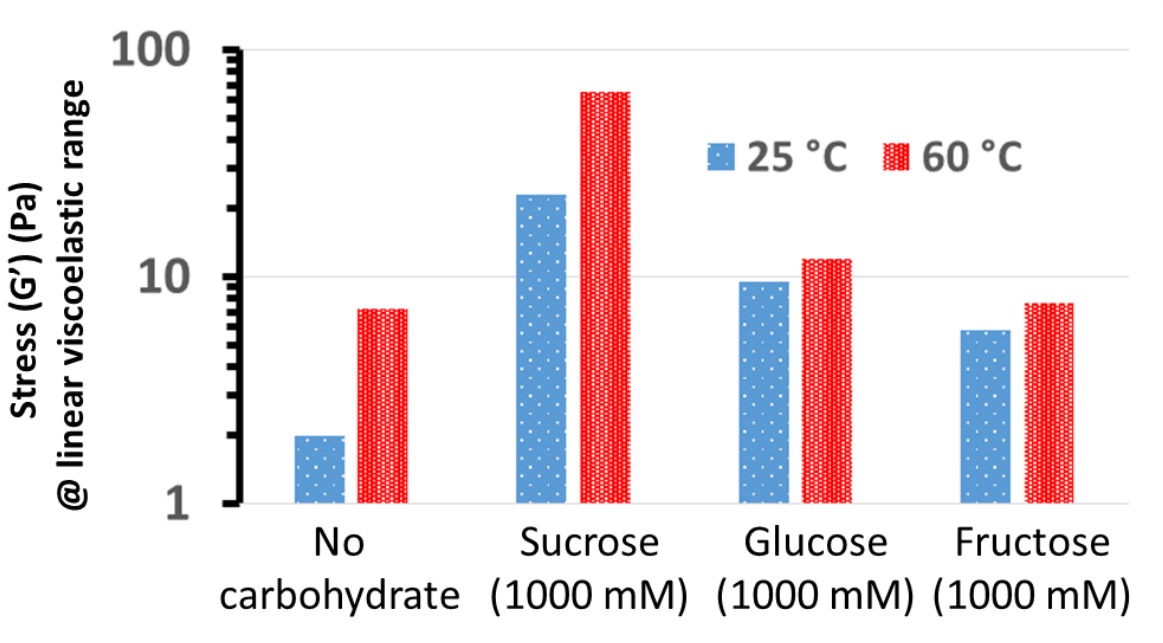

Fig. S15. Storage modulus (G') value at linear viscoelastic range at constant angular frequency (ω = 0.1 rad/s) measured with CTAB based MBG prepared with only water, glucose, sucrose and fructose (1000 mM) solution having n-pentanol as co-surfactant formed at T = 25 °C and 60 °C. Experimental condition: [CTAB] = 50 mM, z= 10, W_0 = 120.

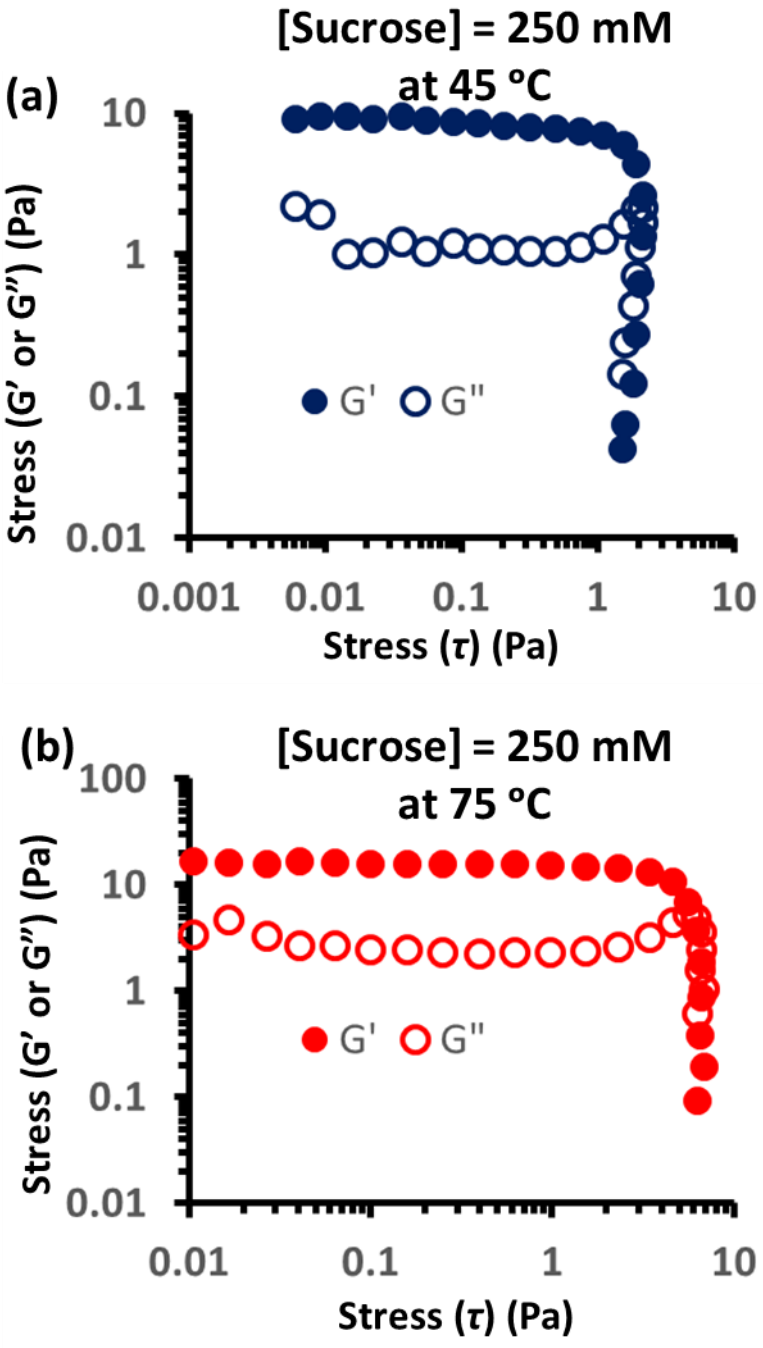

Fig. S16. Plot of storage modulus (G') and loss modulus (G") as a function of oscillatory stress at constant angular frequency (ω = 0.1 rad/s) measured with CTAB based MBG prepared with sucrose (250 mM) solution having n-pentanol as co-surfactant formed at T = 45 °C and 75 °C. Experimental condition: [CTAB] = 50 mM, z = 10, W_0 = 120.

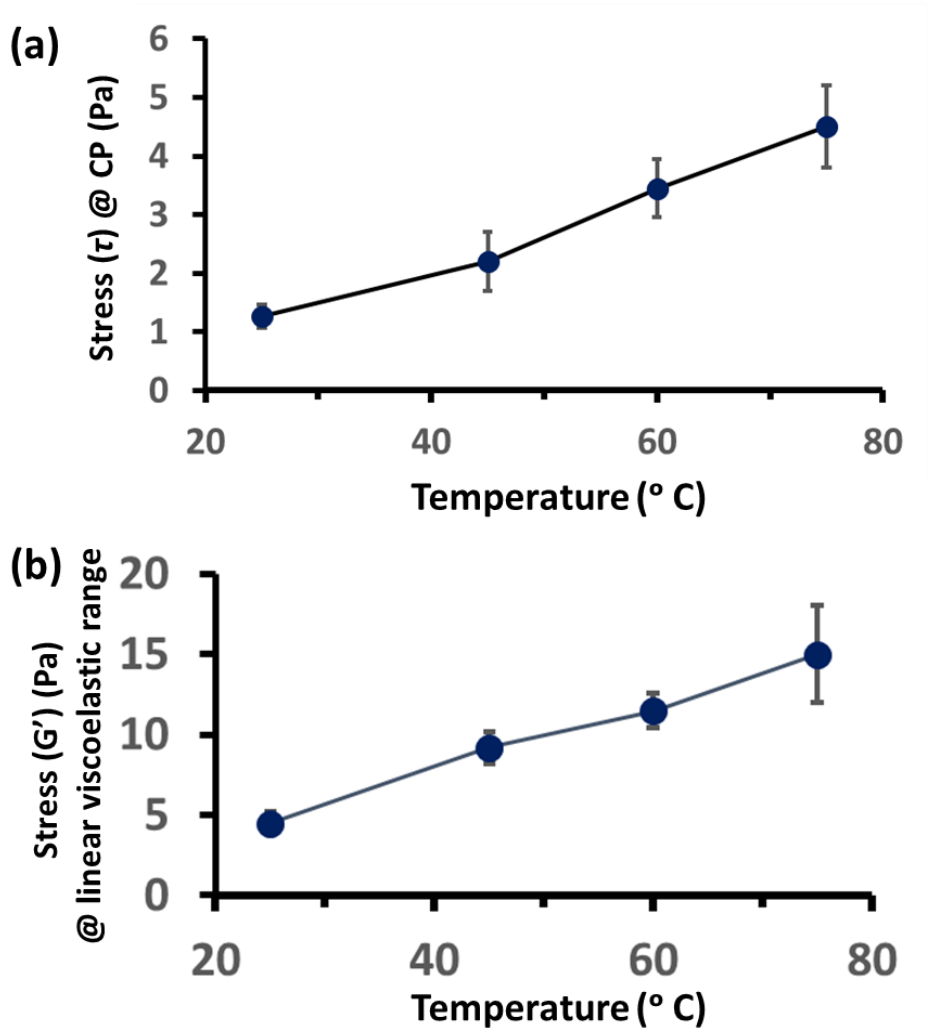

Fig. S17. (a) Storage modulus (G') value at linear viscoelastic range at constant angular frequency (ω = 0.1 rad/s) and (b) Oscillatory stress at G' and G" crossover point (CP) measured with CTAB based MBG prepared with sucrose (250 mM) solution having n-pentanol as co-surfactant formed at T = 25 °C, 45 °C, 60 °C and 75 °C. Experimental condition: [CTAB] = 50 mM, z= 10, W_0 = 120.

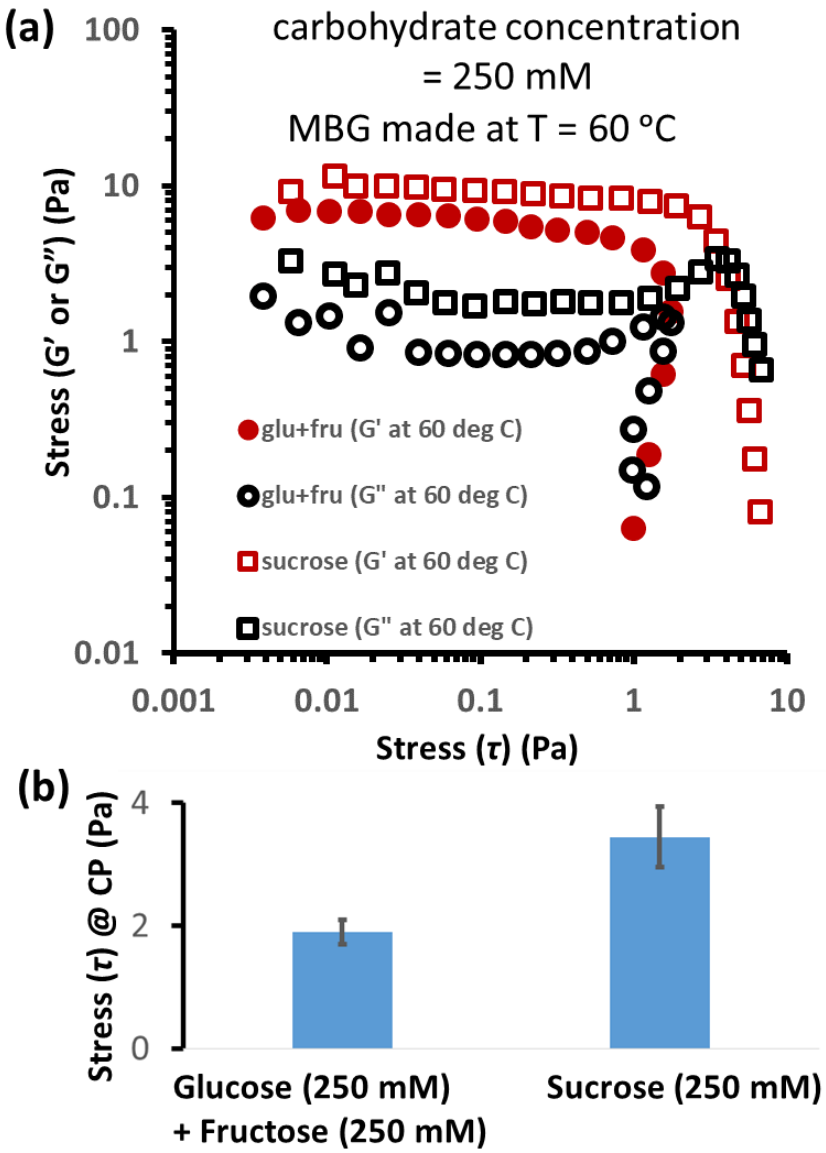

Fig. S18. (a) Plot of storage modulus (G') and loss modulus (G") as a function of oscillatory stress at constant angular frequency (ω = 0.1 rad/s) measured with CTAB based MBG prepared with glucose (250 mM) + fructose (250 mM) solution (and with sucrose (250 mM) solution for comparison) having n-pentanol as co-surfactant formed at T = 60 °C. Experimental condition: [CTAB] = 50 mM, z = 10, W_0 = 120. (b) Comparison of Oscillatory stress at G' and G" crossover point (CP) measured with CTAB based MBG prepared with sucrose (250 mM) solution and glucose(250 mM) + fructose (250 mM) solution having n-pentanol as co-surfactant formed at T = 60 °C. Experimental condition: [CTAB] = 50 mM, z= 10, W_0 = 120.

This experiment suggests that heated MBG formed with sucrose (250 mM) solution is stronger than when MBG made with glucose (250 mM) + fructose (250 mM) solution. This is worthy to mention sucrose is made up of glucose and fructose connected with (β1-->2) glycosidic linkage. This is due to the multivalent binding or accumulated multiple affinities of hydroxyl group in sucrose compared to glucose and fructose.[S1]

7. Fluorescence Microscopic images:

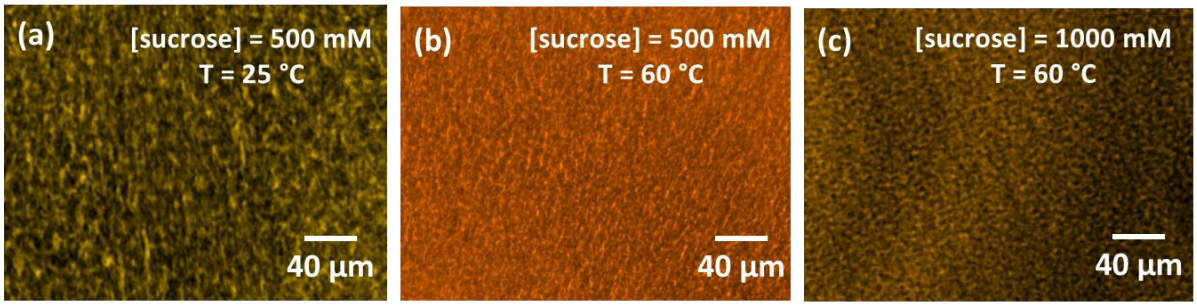

Fig. S19. (a-c) Fluorescence microscopic images of MBG made of sucrose solution (500 and 1000 mM) at T = 25 °C and 60 °C. Fluorescence images were taken by using nile red dye (10 µM). Expt condition: [CTAB] = 50 mM, W_0 = 120. Fluorescence images were taken by using nile red dye (10 µM).

8. Transmission Electron Microscopic (TEM) images:

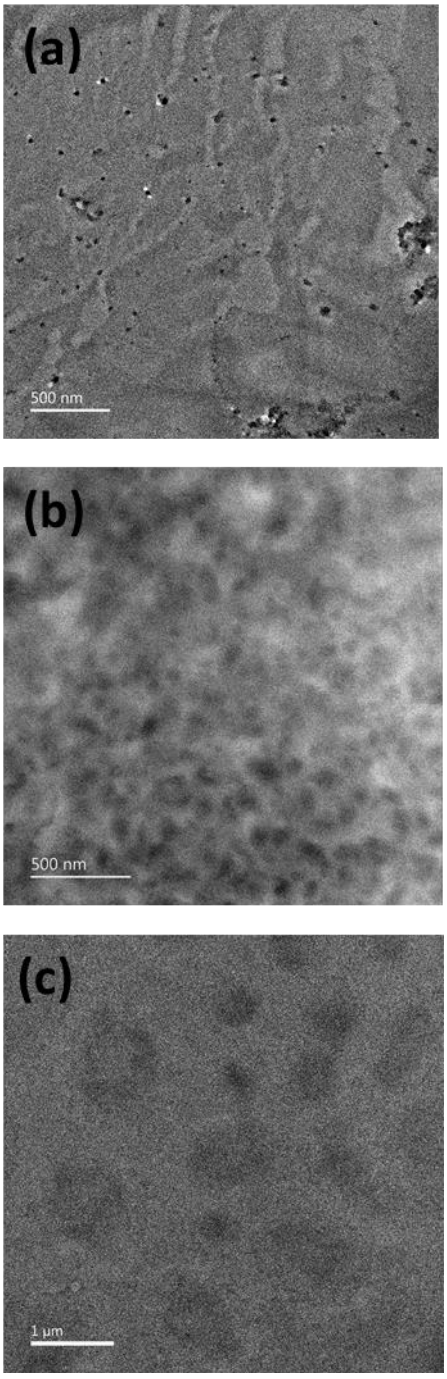

Fig. S20. TEM images of MBG made of (a) water, (b) sucrose (250 mM) and (c) sucrose (500 mM) solution.

9. Optical Microscopic images:

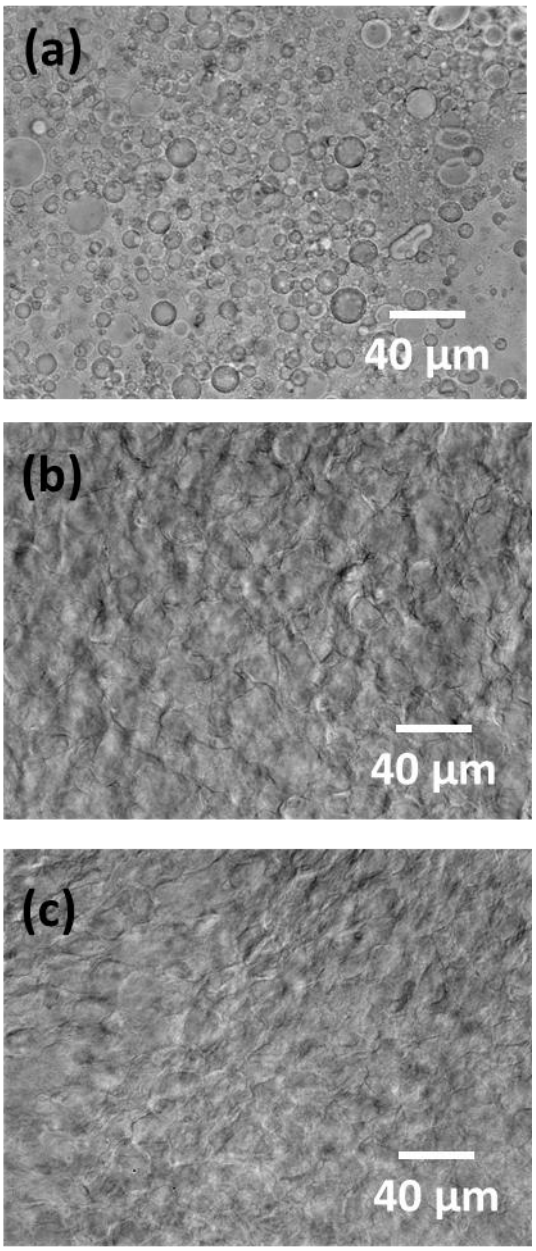

Fig. S21. Optical microscopic images of microemulsion before forming gel made of (a) water, (b) sucrose (250 mM) and (c) sucrose (500 mM) solution. . Experimental condition: [CTAB] = 50 mM, isooctane as oil phase and pentanol as co-surfactant, z = 10, W_0 = 90.

10. Enzyme localization studies:

Fluorescence spectroscopy:

To prove the localization of enzymes in the reverse miceller domain, at first we have performed fluorescence spectroscopic experiments as shown in Fig. S22. We have monitored the tryptophan emission of the enzymes by exciting at 285 nm in three different systems, namely- in pure water, in CTAB micelle and CTAB reverse micelle. In case of HRP and α-glucosidase, the spectral pattern is different for CTAB micelle and reverse micelle compared to water and in both the cases red shift of peak maxima were observed in comparison to water, probably due to interaction with CTAB headgroup. In contrary, for trypsin, almost identical spectra was observed in each cases. It suggests that HRP and α-glucosidase have a tendency to bind with CTAB headgroup in both miceller and reverse miceller media, which also signifies interfacial localization of HRP and α-glucosidase in case of reverse micelle. However, trypsin being a positive charged protein tends to stay away from the cationic CTAB head group thus in reverse miceller media it also prefers to remain in the water pool.

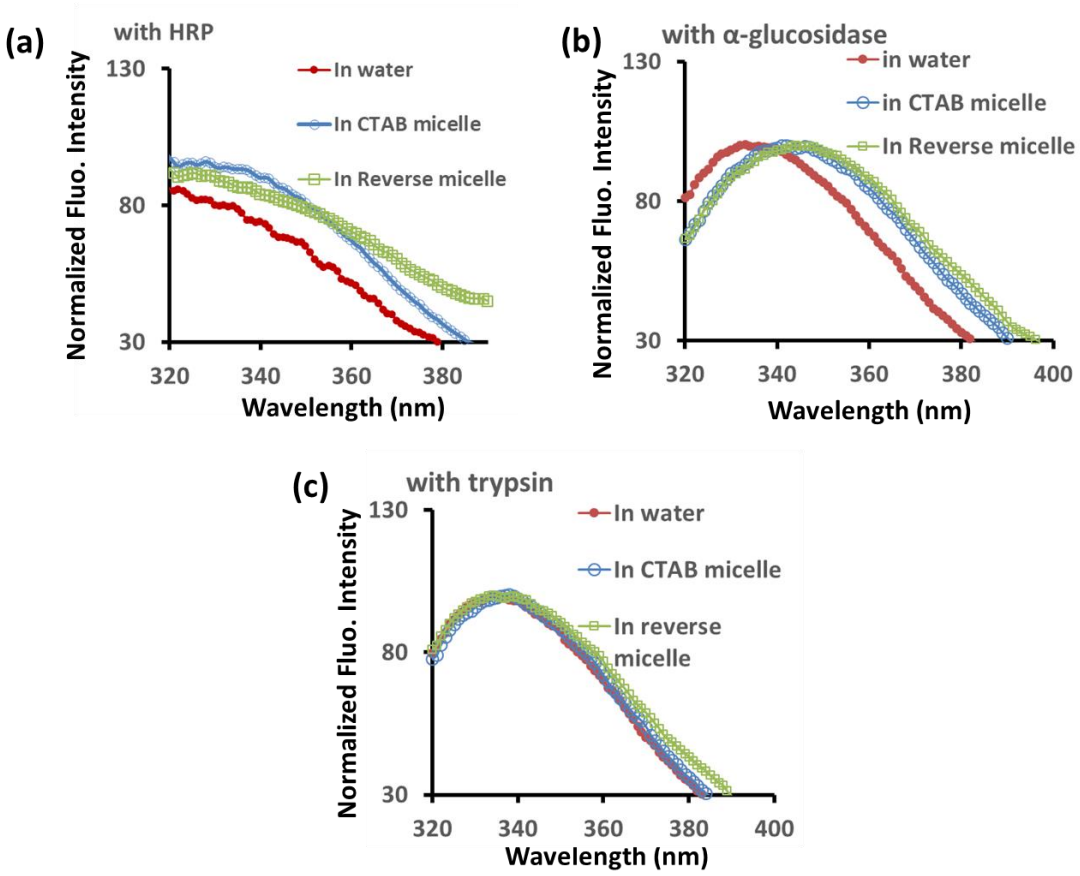

Fig. S22. Fluorescence spectra of (a) HRP, (b) α-glucosidase and (c) trypsin in water, CTAB micelle and CTAB reverse miceller media. Enzyme concentration was maintained at 5 μM in each cases. Concentration of CTAB in CTAB micelle was 2 mM (CMC of CTAB is 0.9 mM)[S2] to ensure miceller form. For reverse micelle, [CTAB] = 50 mM, n-pentanol was used as co-surfactant, z = 10, W_0 = 48. Excitation wavelength: 285 nm, ex/em slit width = 10/10 nm.

Fluorescence microscopy:

For direct visualization of the enzyme localization in microemulsion and sucrose-mediated microemulsion based gel system, we have first fluorescently labelled HRP and α-glucosidase with fluorescein isothiacyanate (FITC).

Synthesis of FITC tagged HRP and α-glucosidase:

FITC-tagged HRP and α-glucosidase have been prepared in a similar manner as reported in literature.[S3] 2 mg/mL enzyme solution was dissolved in sodium carbonate buffer pH 9.0 at room temperature. Then FITC (1mg/ml) was dissolved in DMSO (freshly prepared). 200 µL FITC solution was slowly added to the enzyme solution and covered with aluminium foil and kept at 4 °C for 4 h. The reaction was quenched by ammonium chloride solution (final concentration of it was kept at 50 mM). The vial was kept at 4 °C for 2 h. The above prepared conjugation was then purified by gel filtration (Sephadex G-25), using 5 mM phosphate buffer (pH 8).

UV scan spectra of fractions obtained above were taken and it was observed that HRP-FITC showed peaks at 403 nm (soret peak of HRP) and 495 nm (for FITC), whereas α-glucosidase-FITC conjugate showed peaks at 280 nm and 495 nm (for FITC). Tagging efficiency for HRP and α-glucosidase were almost 0.35 and 0.9 (dye/protein), respectively.

The dye/protein ratio (D/P) of the bioconjugate was calculated by the following formula $D/P = (A_{max}/\varepsilon_{dye}) \times (\varepsilon_{protein}/A_m)$, where $A_m = A_{280}\text{-}c.A_{max}$ (for α-glucosidase -FITC conjugate) and A_{410} for HRP-FITC conjugate.

Here, A_{280} is the absorbance of the α-glucosidase-FITC conjugate at 280 nm; A_{403} is the absorbance of the HRP-FITC conjugate at 403 nm, A_{max} is the absorbance of the conjugate at the absorption maximum of the corresponding FITC, c is the correction factor (c = 0.29) for α-glucosidase-FITC conjugate; ε_{HRP} (at 403 nm), $\varepsilon_{\alpha\text{-glucosidase}}$ (at 280 nm) and ε_{FITC} (at 495 nm) are the molar extinction coefficients for the enzymes and the fluorophore which are 102000 $M^{-1}cm^{-1}$, 130650 $M^{-1}cm^{-1}$ and 68000 $M^{-1}cm^{-1}$respectively.[S3-S5]

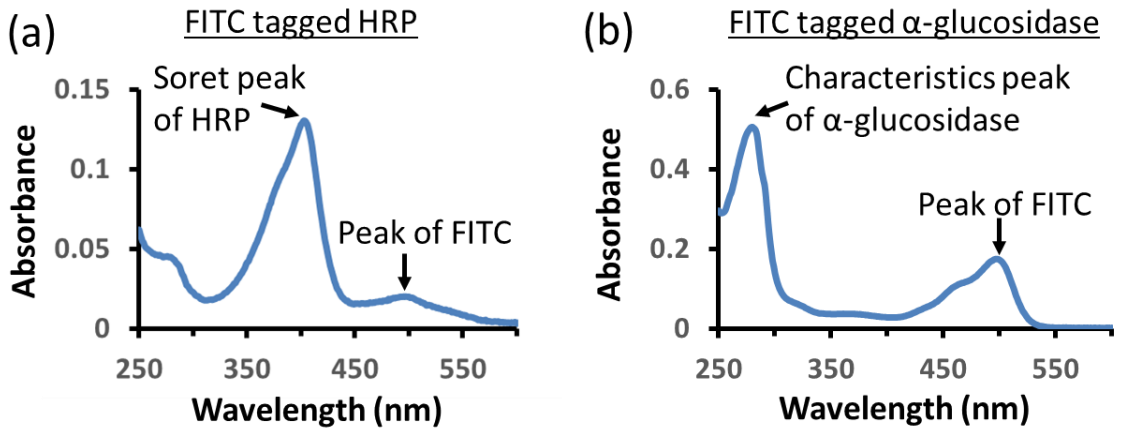

Fig. S23. UV- Vis spectra of a) HRP-FITC b) α-glucosidase–FITC conjugate.

Fluorescence microscopic images

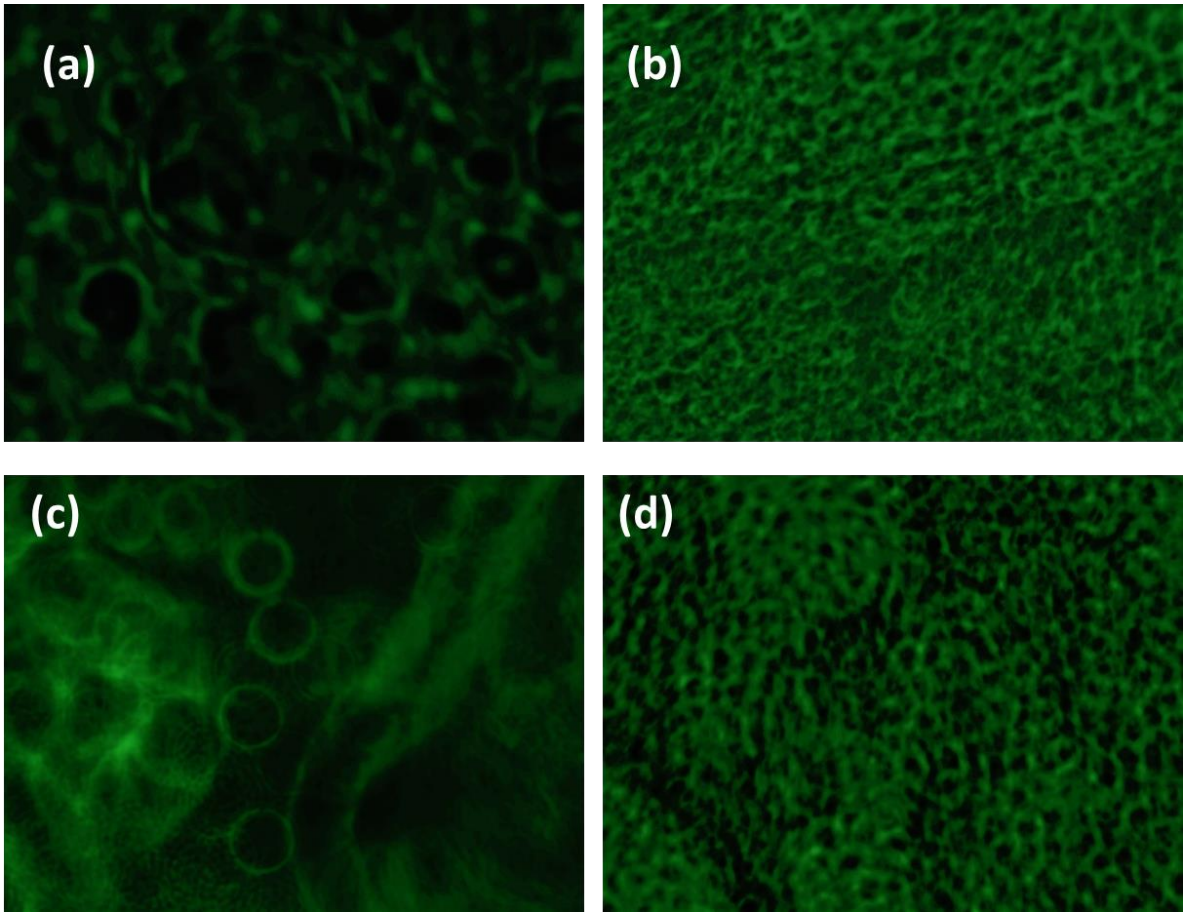

Fig. S24. Fluorescence microscopic images FITC-HRP conjugate containing (a) microemulsion before forming gel and (b) microemulsion based gel and FITC-α-glucosidase conjugate containing (c) microemulsion before forming gel and (d) microemulsion based gel. Experimental condition in microemulsion before forming gel are [CTAB] = 50 mM, isooctane as oil phase and pentanol as co-surfactant, z = 10, W_0 = 80; and in microemulsion based gel W_0 = 120, whereas other factors are same. Enzyme concentration was kept at 5 µM in all instances. Images in the (a) and (c) compartment were taken in 40 X lens and x-axis of each images are 176 µm, whereas Images in the (b) and (d) compartment were taken in 20 X lens and x-axis of each images are 352 µm.

Additionally, we have also performed fluorescence spectroscopic experiments with both FITC-HRP and FITC-α-glucosidase conjugates by exciting at 485 nm (which is the excitation maxima of FITC) in water, CTAB micelle and CTAB reverse micelles. Here also identical spectra was observed in CTAB micelle and reverse micelle in comparison to water, which suggests localization of the enzymes in the interfacial domain of reverse micelle. The results are almost similar to what we have observed in Fig. S22 with native enzymes.

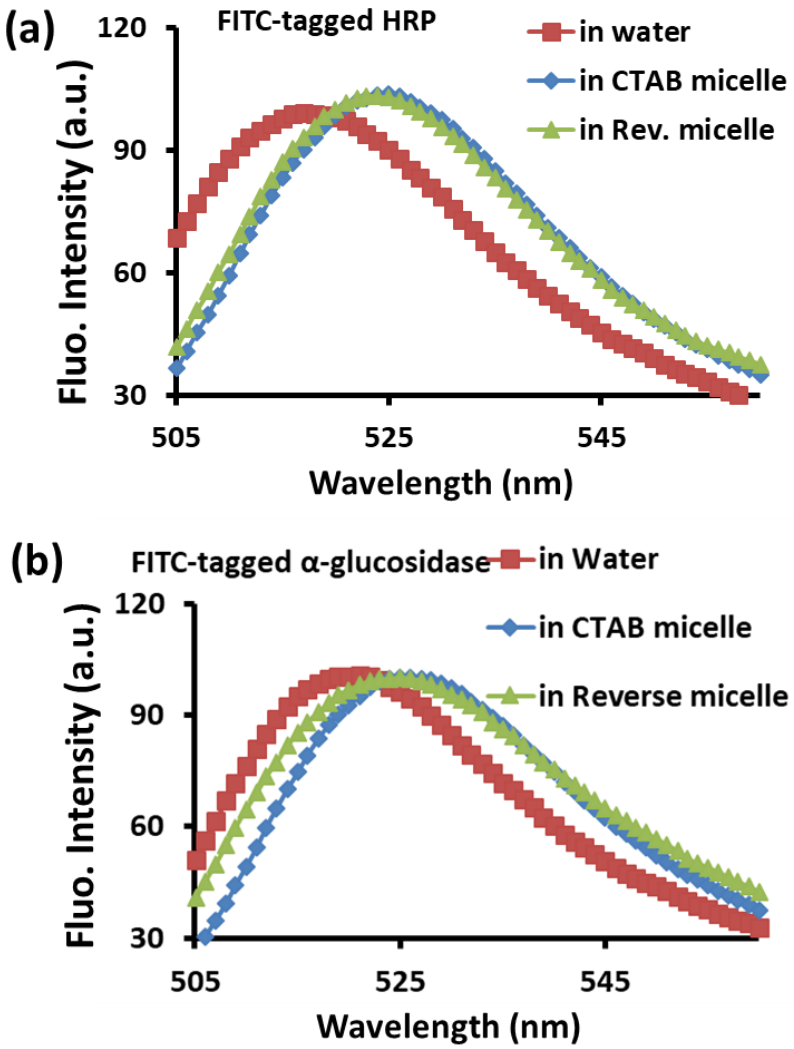

Fig. S25. Fluorescence spectra of (a) FITC-HRP conjugate (HRP concentration = 0.5 μM) and (b) FITC-α-glucosidase conjugate (α-glucosidase concentration = 0.5 μM) in water, CTAB micelle and CTAB reverse miceller media. Concentration of CTAB in CTAB micelle was 2 mM (CMC of CTAB is 0.9 mM)[ref] to ensure miceller form. For reverse micelle, [CTAB] = 50 mM, n-pentanol was used as co-surfactant, z = 10, W_0 = 48. Excitation wavelength: 285 nm, ex/em slit width = 5/5 nm.

The above experiments clearly demonstrate the localization of the enzymes (HRP and α-glucosidase) in the interfacial region.

11. Enzyme entrapment study:

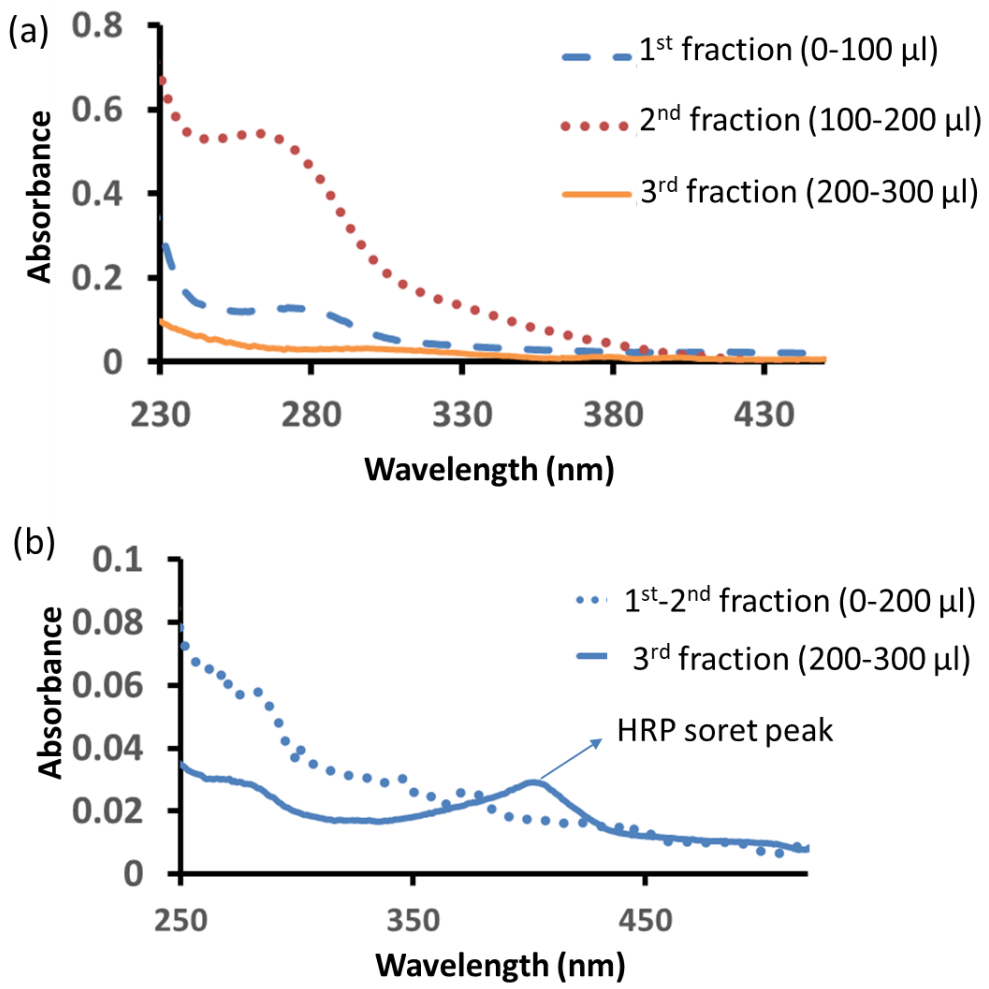

Fig. S26. UV-spectra of different collected fractions of eluted (a) trypsin and (b) HRP through the MBG column when only trypsin or HRP was passed through it. 100 ul of water/ethanol (1:1) solution of trypsin or HRP having 60 µM concentration was passed through MBG of 5.5 ml in the column. In the MBG, oil phase is isooctane, [CTAB] = 50 mM, [sucrose] = 250 mM, z = 10 (n-pentanol as co-surfactant), W_0 = 120.

From the above fig. S22, it is clear that trypsin being a water-pool solubilized enzyme passed through the column easily and almost all the trypsin gets eluted within 200 µl of eluted fraction. In contrary, HRP started to elute only in minor fraction after 200 µl of eluted fraction through the column. This clearly suggest that HRP being an interfacially solubilized enzyme has much higher propensity to get entrapped inside the column.

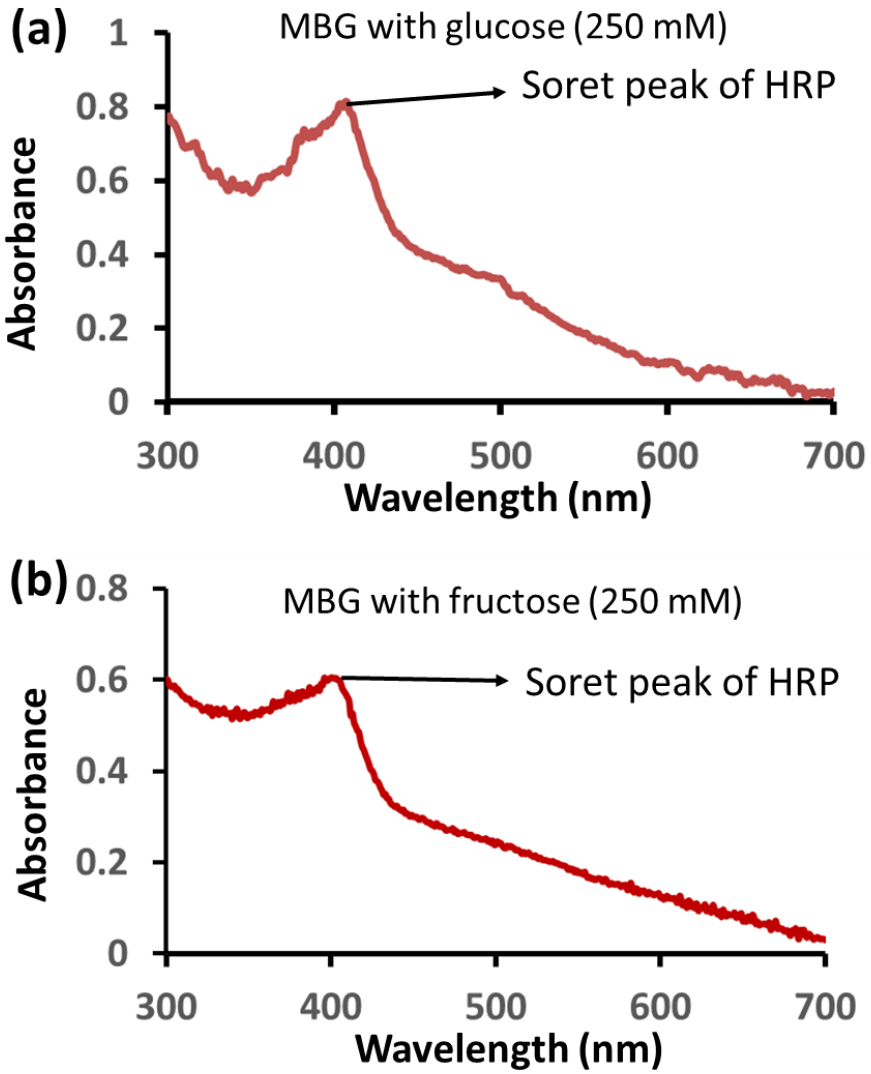

Fig. S27. UV-spectra of collected fractions of eluted HRP through the MBG column when only HRP solution was passed through it. 100 ul of water/ethanol (1:1) solution of HRP having 60 µM concentration was passed through MBG of 5.5 ml in the column. In the MBG, oil phase is isooctane, [CTAB] = 50 mM, [sucrose] = 250 mM, z = 10 (n-pentanol as co-surfactant), W_0 = 120.

This data suggests that glucose (250 mM) or fructose (250 mM) based MBG are not strong enough to entrap HRP like sucrose based MBG.

12. Catalytic activity of HRP in water and reverse micelle in absence and presence of carbohydrates

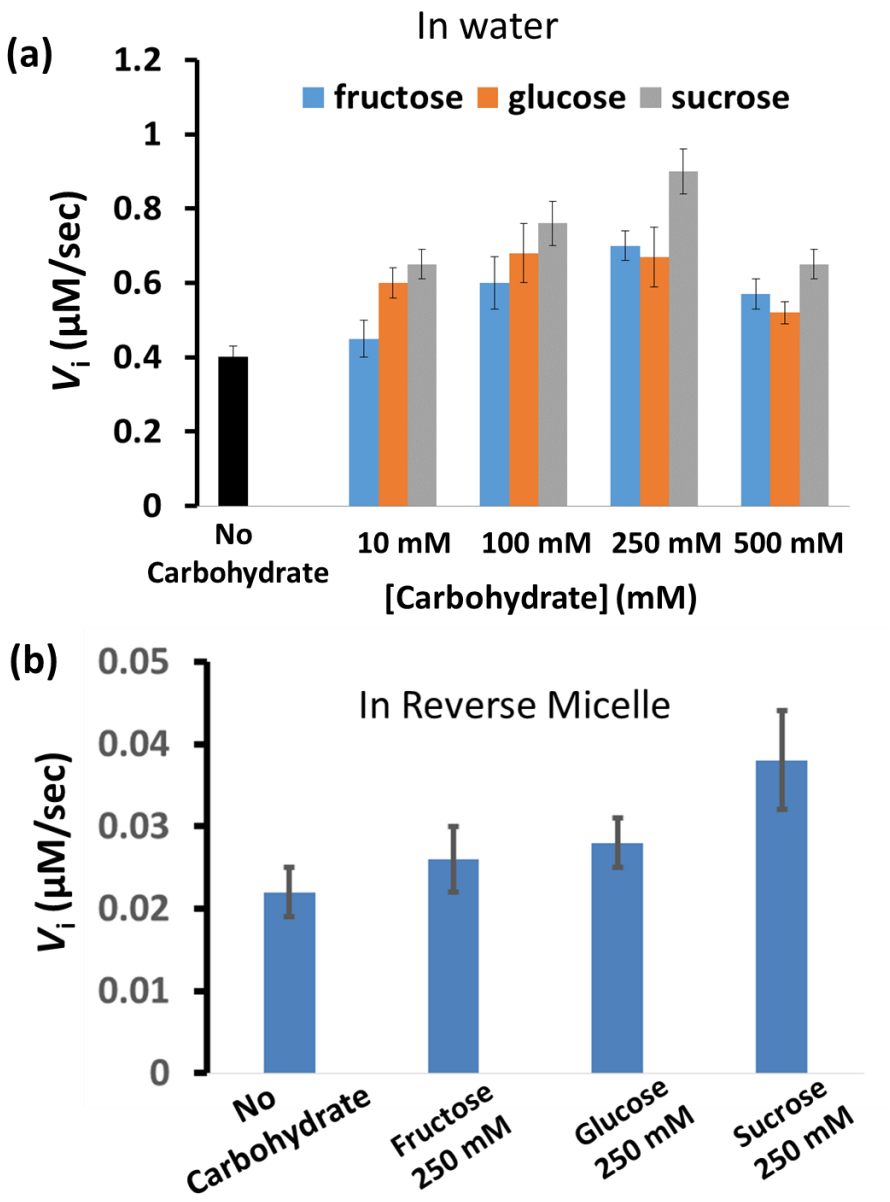

Fig. S28. (a) Initial rate (V_i) of HRP catalysis at fixed substrate (ODA) concentration (100 µM) and [H_2O_2] = 100 µM in presence of HRP (0.25 µM) as a function of varying carbohydrate concentration (0-500 mM) in water. (b) Initial rate (V_i) of HRP catalysis at fixed substrate (ODA) concentration (100 µM) and [H_2O_2] = 100 µM in presence of HRP (0.3 µM) at fixed carbohydrate concentration (250 mM). For reverse micelle, [CTAB] = 50 mM, n-pentanol as co-surfactant, z = 10, W_0 = 24.

Calculation of the reaction product was calculated by following molar extinction co-efficient value of 11300 $M^{-1}cm^{-1}$, of oxidized ODA at 440 nm.[S6] In reverse micelle, only 250 mM carbohydrate solution was used as it was found that in water highest activity was observed when 250 mMcarbohydrate solution were used.

13. MBG packed columnar catalysis using HRP:

Methods: 5.5 ml MBG was packed in the column as shown in Fig. S25. Then, 100 µl, HRP having 60 µM concentration was allowed to soak in the MBG of 5.5 ml in the column. Next, required amount of water or water/ethanol solution having substrates ODA or TMP (1 mM) and [H_2O_2] = 1 mM, have been poured in the column. Then the eluted solution (which is also ~100 µl) collected until the last drop (which takes around 5 min). This process has been done 5-6 times. Then this collected fraction of the solution was diluted up to 1 ml using either water or water/ethanol and their UV absorbance spectra was taken. From the molar extinction coefficient of the products at respective wavelength (for ODA at 440 nm and for TMB at 460 nm), calculation of the reaction yield was done.

For catalysis in MBG we have observed 250 mM sucrose solution formed MBG heated at 60 °C is the most preferred one as it can entrap HRP with subsequent period of time and also the solution containing the product eluted easily. We have observed in stronger gel (for e.g. MBG formed by using 500 or 1000 mM sucrose) the elution of the product through gel is very time consuming, even it takes 1-2 hours to elute one drop of the solution (for 1000 mM sucrose mediated MBG) added on top of the column, although enzyme retention ability will be much higher in this case.

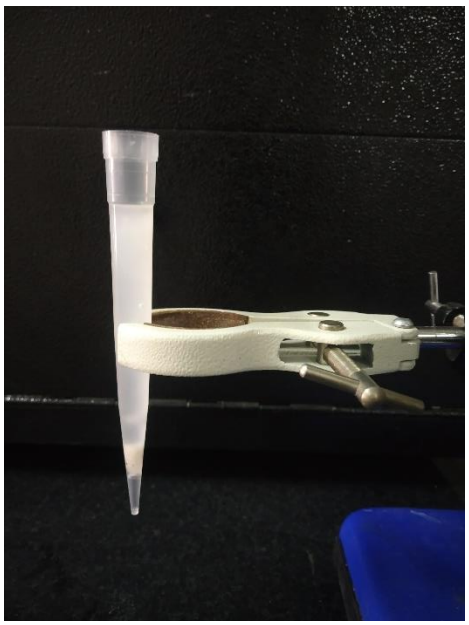

Fig. S29. Representative photograph of the MBG (made with sucrose (250 mM) solution) packed column used in this study for HRP entrapment and catalysis.

ODA as substrate:

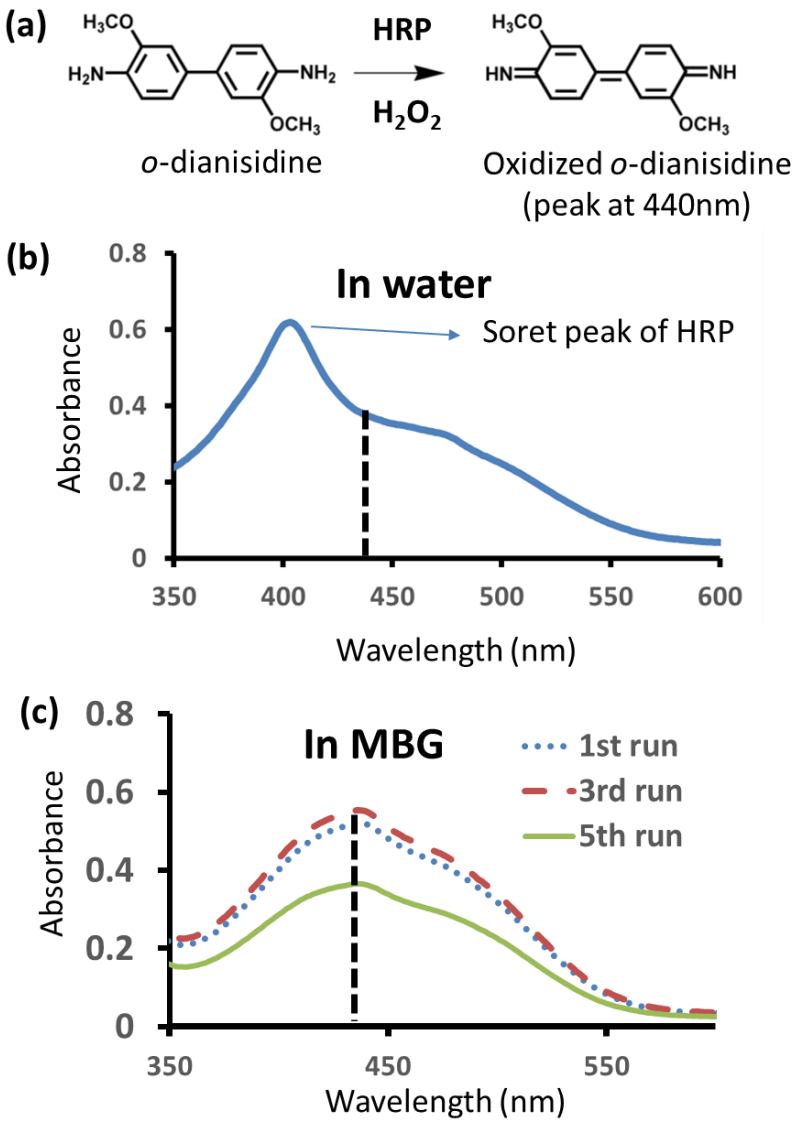

Fig. S30. (a) Structure of the substrate o-dianisidine (ODA) and (HRP+H_2O_2)-oxidized product of ODA. (b) UV-vis spectra of the oxidized ODA when the reaction is carried in water in presence of HRP (1.2 µM), [H_2O_2] = 1 mM, [ODA] = 1 mM. (c) Representative UV spectra of eluted reaction product (oxidized ODA) from MBG, after 1st, 3rd and 5th run. 100 µl, HRP having 60 µM concentration was allowed to soak in the MBG of 5.5 ml in the column. Then 100 µl of water solution having ODA (1 mM) and [H_2O_2] = 1 mM, has been poured in the column having 5.5 ml of MBG and collected until the last drop (which takes around 5 min). This process has been done 5 times. In the MBG, oil phase is isooctane, [CTAB] = 50 mM, [sucrose] = 250 mM, z = 10 (n-pentanol as co-surfactant), W_0 = 120.

The eluted product amount was compared with only water and given in Figure 4c of the main manuscript.

Notably, in the eluted solution from the MBG, no peak of HRP (denoted by soret band at 403 nm) has been detected. It clearly suggests that HRP has been retained inside the column.

TMB as substrate:

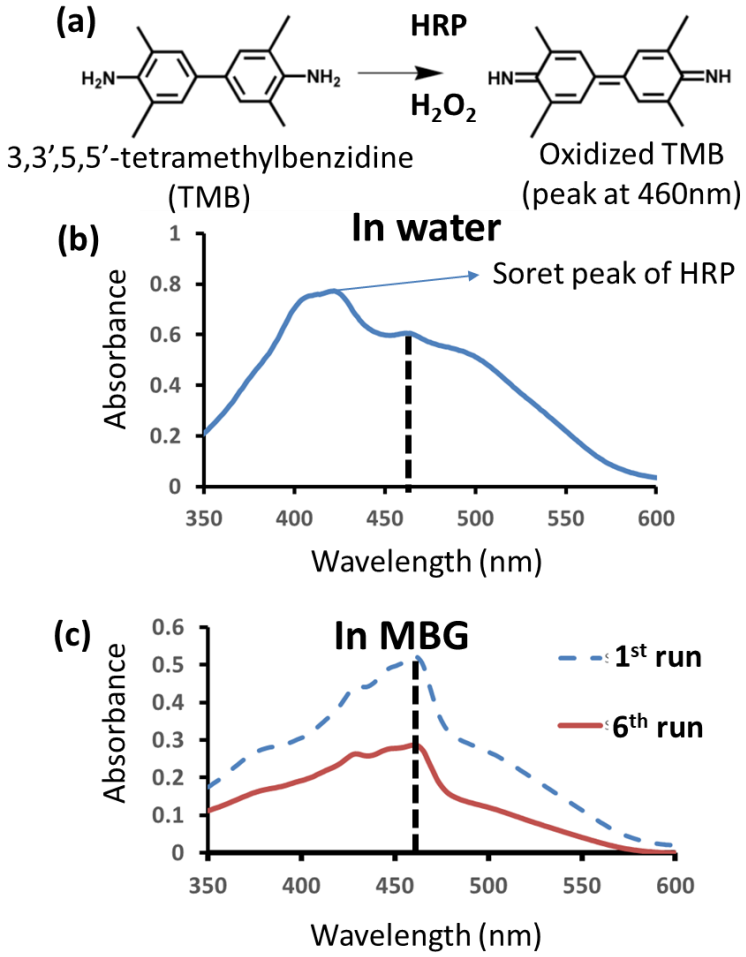

Fig. S31. (a) Structure of the substrate TMB and (HRP+H_2O_2)-oxidized product of TMB. (b) UV-vis spectra of the oxidized TMB when the reaction is carried in water in presence of HRP (1.2 µM), [H_2O_2] = 1 mM, [TMB] = 1 mM. (c) Representative UV spectra of eluted reaction product (oxidized TMB) from MBG, after 1st and 6th run. 100 µl, HRP having 60 µM concentration was allowed to soak in the MBG of 5.5 ml in the column. Then 100 µl of ethanolic solution having TMB (1 mM) and [H_2O_2] = 1 mM, has been poured in the column having 5.5 ml of MBG and collected until the last drop (which takes around 5 min). This process has been done 5 times. In the MBG, oil phase is isooctane, [CTAB] = 50 mM, [sucrose] = 250 mM, z = 10 (n-pentanol as co-surfactant), W_0 = 120.

Calculation of the reaction product was calculated by following molar extinction co-efficient value of 59000 $M^{-1}cm^{-1}$, of oxidized TMB at 460 nm.[S7] The eluted product amount was compared with only water and given in Figure 4c of the main manuscript.

Notably, in the eluted solution from the MBG, no peak of HRP (denoted by soret band at 403 nm) has been detected. It clearly suggests that HRP has been retained inside the column.

ODA and TMB added batchwise sequentially in the MBG through HRP packed column:

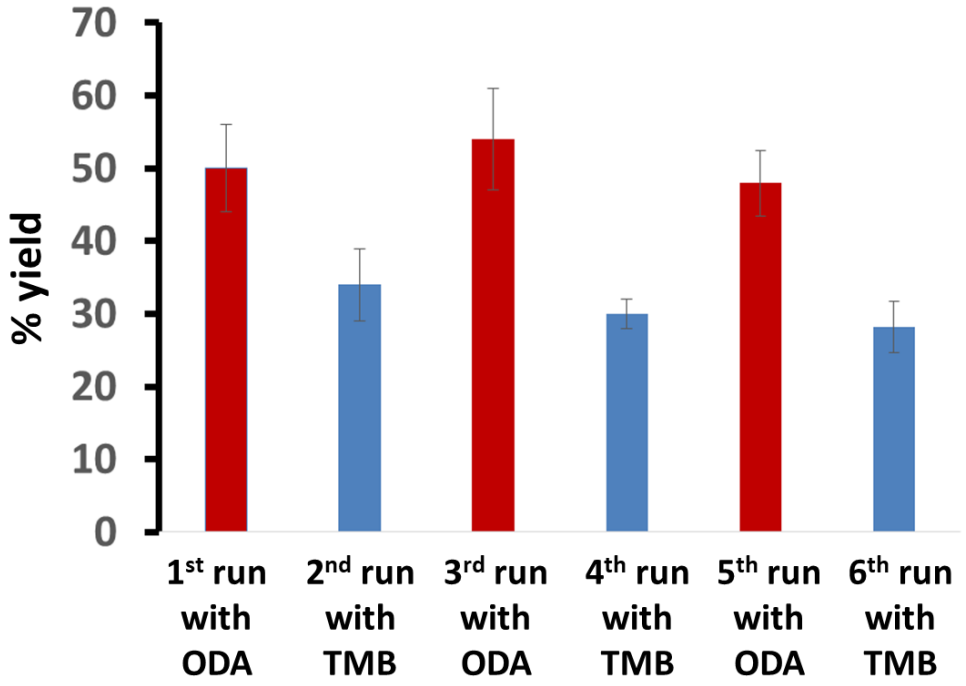

Fig. S32. Yield of the oxidized reaction product after passing ODA (in water) and TMB (in ethanol) substrate solution (100 µl of 1 mM) along with [H_2O_2]= 1 mM through HRP entrapped MBG column ([HRP] = 1.3 µM). Yield is calculated as the average of triplicate experiment.

ODA and TMB added together in the MBG through HRP packed column:

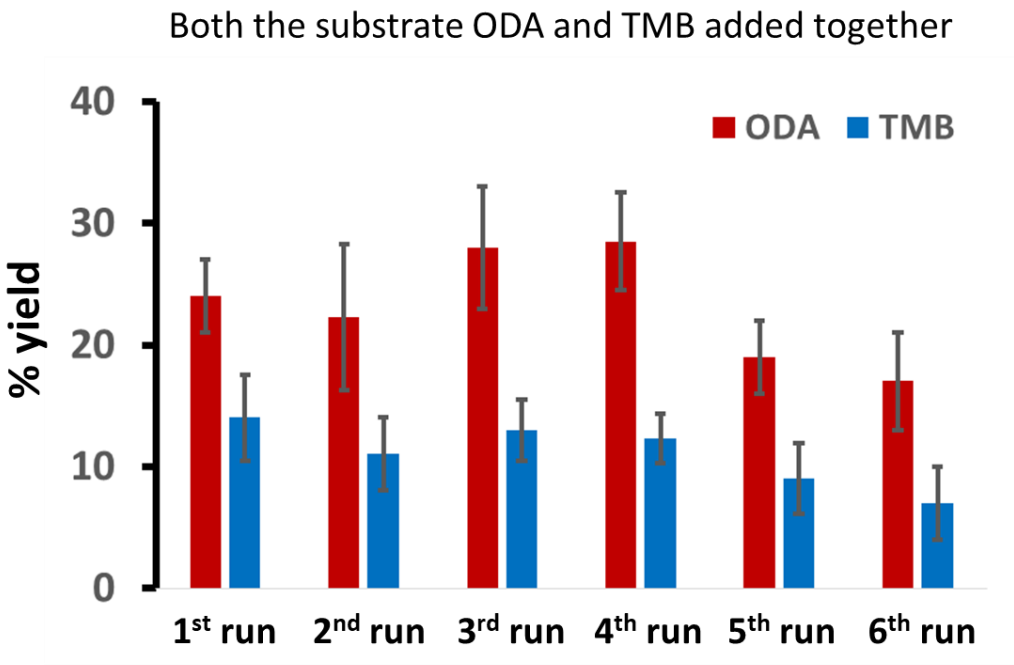

Fig. S33. Yield of the oxidized reaction product after passing ODA (in water) and TMB (in ethanol) substrate solution (100 µl of 0.5 mM each) together at a time along with [H_2O_2] = 1 mM through HRP entrapped MBG column ([HRP] = 1.3 µM). Yield is calculated as the average of triplicate experiment.

Stability of HRP in the sucrose-mediated MBG column:

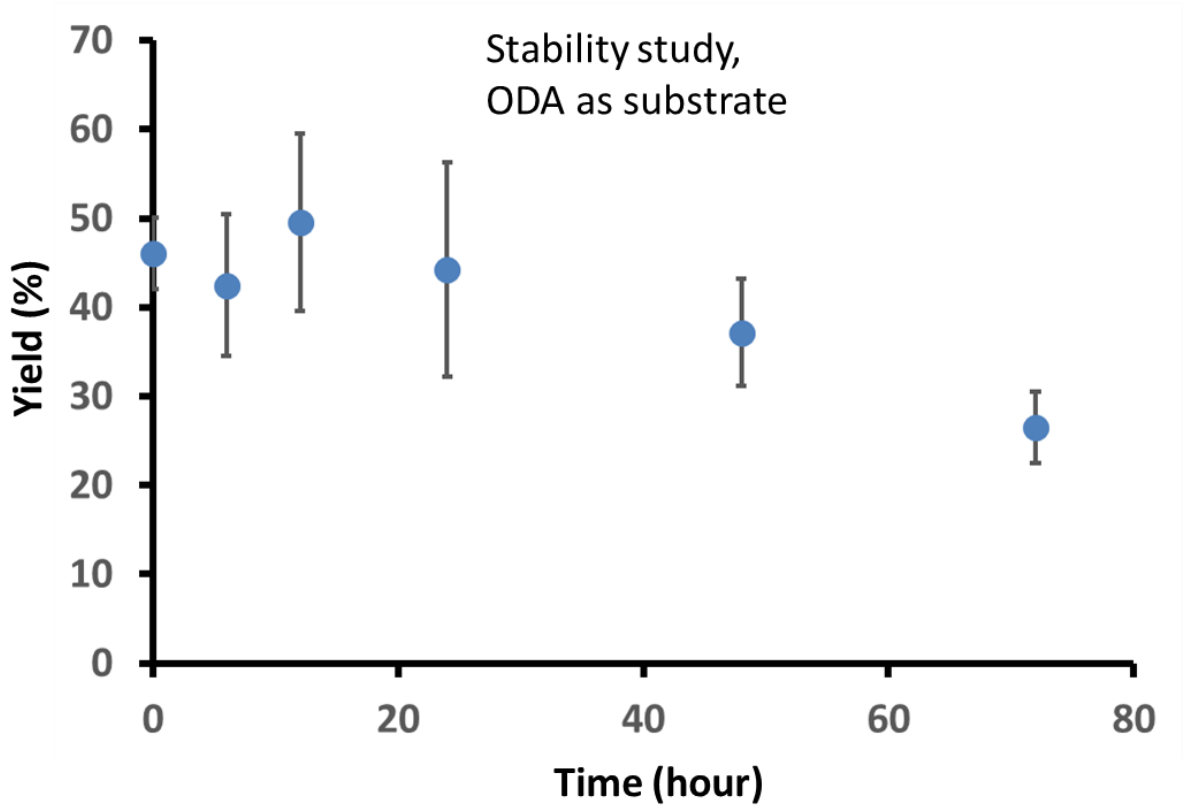

Fig. S34. Yield of the oxidized reaction product after passing ODA (in water) substrate solution (100 µl of 0.5 mM) with [H_2O_2] = 1 mM through HRP entrapped MBG column ([HRP] = 1.3 µM) at different time interval. Yield is calculated as the average of duplicate experiment.

This study suggests that HRP remains in the column as well as show activity up to 48 hr and after that it subsides.

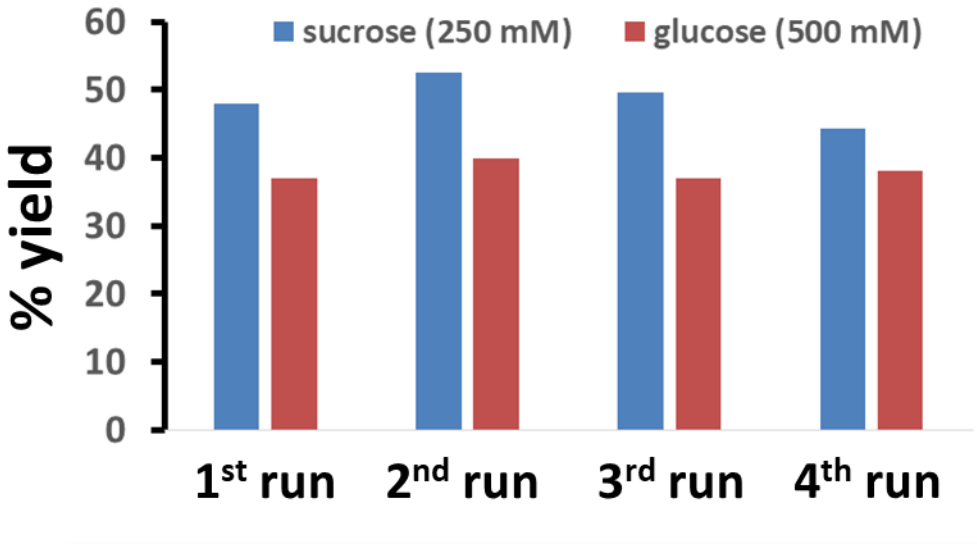

Fig. S35. Comparison of the yield of the oxidized reaction product after passing ODA (in water) substrate solution (100 µl of 0.5 mM) with [H_2O_2]= 1 mM through HRP entrapped MBG column made with 250 mM sucrose and 500 mM glucose heated at 60 °C ([HRP] = 1.3 µM) at different batchwise run.

As 250 mM glucose comprised MBG is not strong enough to entrap HRP, we have used 500 mM glucose comprised MBG which has comparable strength with 250 mM sucrose comprised MBG (made after heating at 60 °C) (see Fig. 3b of the main manuscript). However, the found activity is slightly lower in case of glucose (500 mM) made MBG. In fact, we have found that sucrose has activating effect towards HRP catalysis both in water and in reverse micelle (see Fig. S24). Thus, although glucose mediated MBG is able to trap HRP, but the activity is lower than sucrose mediated MBG. Also, fructose (250, 500 mM) mediated MBG does not show ability to trap HRP because of its lower strength.

Comparison of sucrose-mediated MBG and agarose-mediated MBG in terms of HRP activity and thermal treatment:

We have also checked the efficacy of the developed sucrose-mediated MBG with previously used agarose-mediated MBG. For that purpose, agarose gel mediated MBG has been prepared following literature protocol (Ref. 5 of the main manuscript). Briefly, 2 wt % (40 mg in 2 ml) of agar powder was dissolved in 2 ml of water by heating at 100 °C. It was then mixed with both water-in-oil (100mM (91 mg) AOT was dissolved in 2 ml isooctane with addition of 40 ul water having HRP) and in oil-in-water micro-emulsion (100mM (91 mg) AOT was dissolved in 2 ml water containing HRP with addition of 40 ul isooctane) with final HRP concentration of 1 µM. After that, the mixture was kept for cooling to form the gel.

It was packed in column and 50 µl of 1 mM ODA and 1 mM H_2O_2 were added for monitoring HRP catalysis for six times.

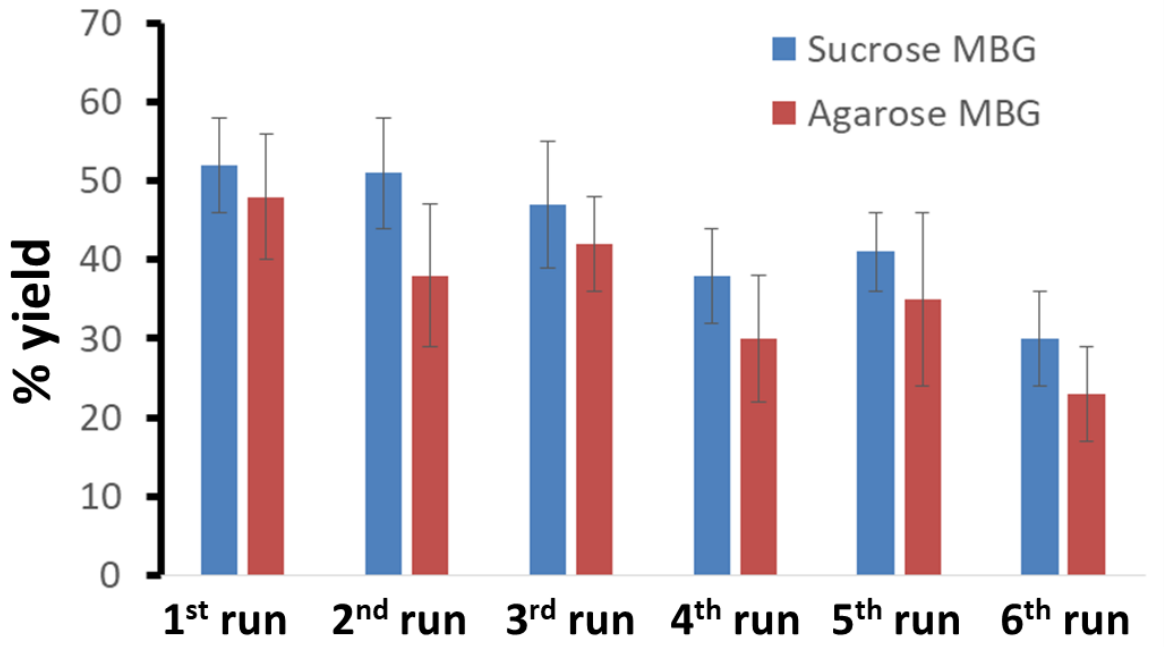

Fig. S36. Yield of the oxidized reaction product after passing ODA (in water) substrate solution (50 µl of 1 mM) along with [H_2O_2] = 1 mM through HRP entrapped MBG column ([HRP] = 1.0 µM). Yield is calculated as the average of duplicate experiment.

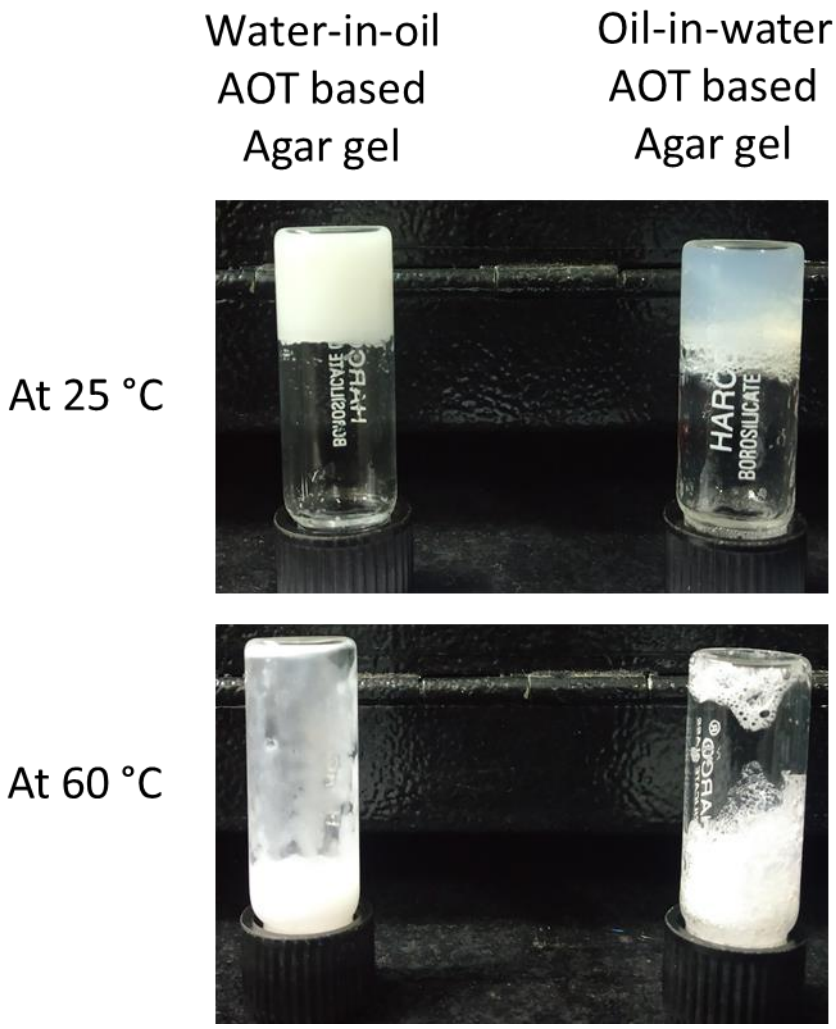

Fig. S37. Optical images of inverted vials of water-in-oil AOT based agar gel and oil-in-water AOT based agar gel at 25 °C and 60 °C.

Fig. S36 suggested that the yield is almost comparable in both sucrose mediated CTAB-MBG and agarose based oil-in-water MBG, whereas the activity for substrate ODA is slightly better in sucrose mediated CTAB-MBG. Also in every run, it took almost 30 min for eluting all the solvents in case of ODA, whereas for sucrose (250 mM) mediated MBG can elute ODA solution and corresponding products in 5-6 min under similar experimental condition. Apart from that, oil-in-water agar MBG is even slower in passing ethanol solubilized TMB solution (almost more than 1.5 h needed to complete one run) which restricts us to use HRP catalysis for organic solvent solubilized TMB substrate in oil-in-water agar MBG.

However, agarose MBG is not thermally stable and upon heating at 60 °C, it loosens its strength and gel property gets lost (Fig. S37). Thus, thermal stiffening property made sucrose mediated MBG unique and also made it suitable candidate as host for thermophilic enzymes.

14. MBG packed columnar catalysis using alpha- glucosidase:

Here, we have used *p*-nitrophenyl-*α*-glucopyranoside as the substrate of the enzyme *α*-glucosidase. The reaction product is p-nitrophenol (PNP) which we have used as the chromophoric agent to monitor the yield of the reaction. For that, we have first determined the molar extinction co-efficient of PNP at 405 nm, in the MBG eluted solution when passed with only 1:1 water-ethanol solution. Molar extinction co-efficient of PNP at 405 nm is 132 $M^{-1}cm^{-1}$. Molar extinction co-eff of PNP is only water is 200 $M^{-1}cm^{-1}$.[S8]

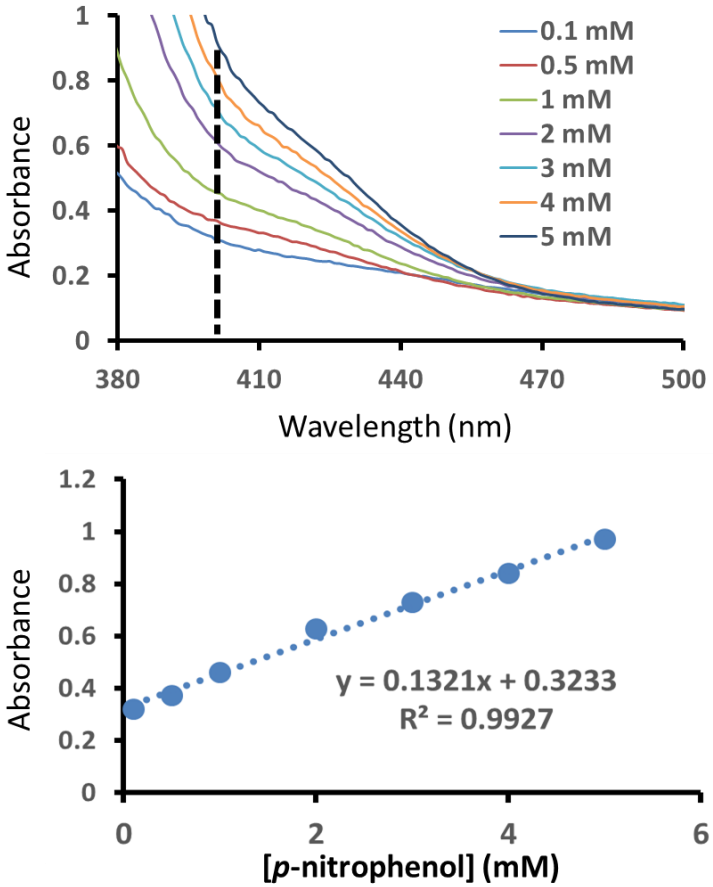

Fig. S38. UV-vis spectra of PNP (0.1-5 mM) in the MBG eluted solution and absorbance (405 nm) of PNP as a function of PNP concentration.

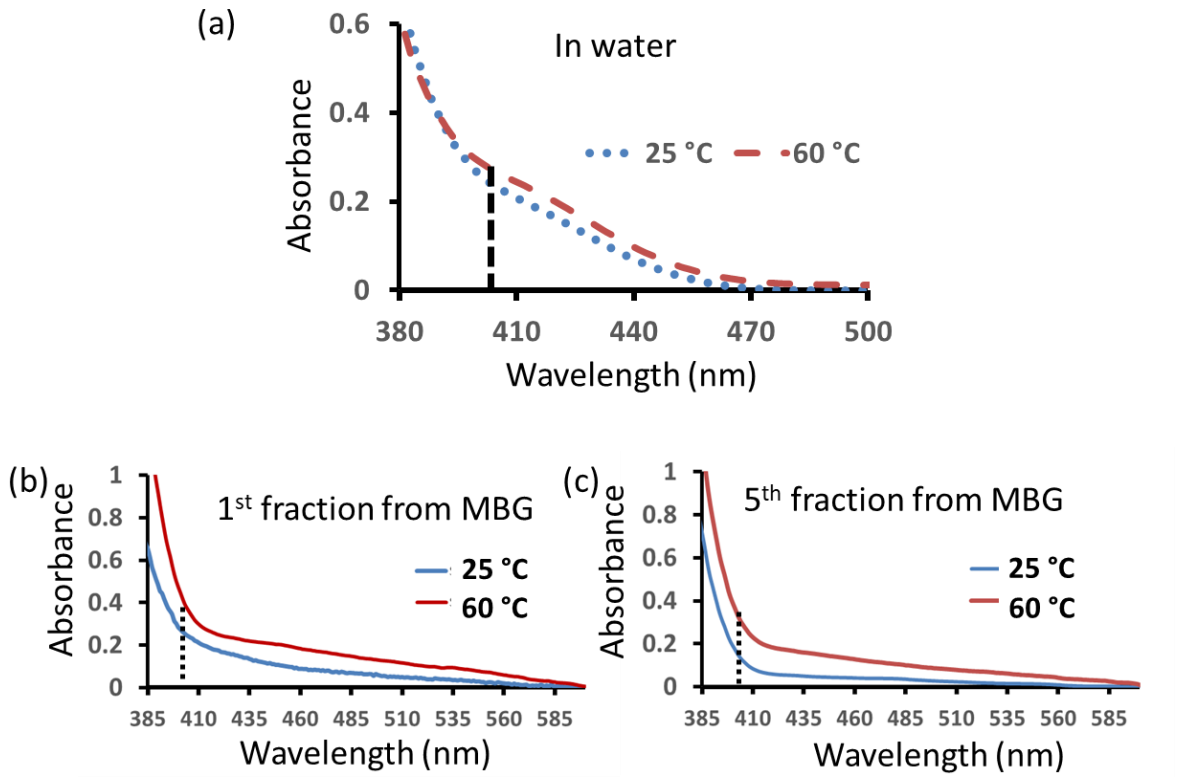

Fig. S39. (a) UV-vis spectra of the reaction product when the reaction is carried in water in presence of α-glucosidase (3 µM), [PNPG] = 5 mM. Representative UV spectra of eluted reaction product from MBG, after 1st and 5th run. 50 µl, α-glucosidase having 320 µM α-glucosidase concentration was allowed to soak in the MBG of 5.5 ml in the column. Then 100 µl of aqueous ethanolic (1:1) solution having PNPG (50 mM), has been poured in the column having 5.5 ml of MBG and collected until the last drop (which takes around 5 min). This process has been done 5 times. In the MBG, oil phase is isooctane, [CTAB] = 50 mM, [sucrose] = 250 mM, z = 10 (n-pentanol as co-surfactant), W_0 = 120.

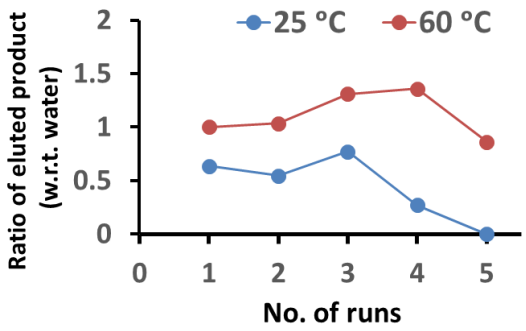

Fig. S40. Ratio of the product yield after passing PNPG (solubilized in ethanol) substrate solution (100 µl of 50 mM) through α-glucosidase entrapped MBG column and after reaction in water solution alone.

12. Captions of supplementary video.

Supplementary video 1 (SV1).

Formation of CTAB-based microemulsion-based gel (MBG) by using *n*-pentanol as co-surfactant and adding water periodically up to W_0 = 100 with constant vortexing. Total volume of the solution = 2 ml, [CTAB] = 50 mM, z = 10 and oil phase isooctane. In the end of the video, at identical experimental condition, when n-heptanol has been used as a co-surfactant, non-formation of gel has been shown.

Supplementary video 2 (SV2).

Formation of CTAB-based microemulsion-based gel (MBG) by using *n*-pentanol as co-surfactant and adding 1000 mM sucrose solution periodically up to W_0 = 120 with constant vortexing. Total volume of the solution = 2 ml, [CTAB] = 50 mM, z = 10 and oil phase isooctane.

13. References.

S1. V. M. Krishnamurthy, L. A. Estroff and G. M. Whitesides, in Multivalency in Ligand Design (Eds.:W. Jahnke, D. A. Erlanson), Wiley-VCH, Weinheim, 2006, pp. 11-53

S2. J. M. Neugebauer, *Methods Enzymol.*, 1990, **182**, 239.

S3. S. Vira, E. Mekhedov, G. Humphrey, P. S. Blank, *Anal. Biochem.* 2010, **402**, 146.

S4. H. Delincée, B. J. Radola, *Eur. J. Biochem.*, 1975, **52**, 321.

S5. S. S. Lee, S. he, S. Withers, *Biochem. J.*, 2001, **359**, 381.

S6. S. Khavari-Nejada and F. Attar, *Biomacromol. J.*, 2015, **1**, 130.

S7. D. J. Triebwasser-Freese, N. Tharayil, C. M. Preston and P. G. Gerard, *Biogeochemistry*, 2015, **124**, 113.

S8. G. N. Bowers, R. B. McComb, R. C. Christensen and R. Schaffer, *Clin. Chem.* 1980, **26**, 724.